Flexural behaviour and design rules for SupaCee sections with web openings

Kajaharan Thirunavukkarasu

Institute of Technology, University of Moratuwa, Homagama, Sri Lanka

Elilarasi Kanthasamy

Faculty of Engineering and Environment, Northumbria University, Newcastle upon Tyne, UK

Keerthan Poologanathan

Faculty of Engineering and Environment, Northumbria University, Newcastle upon Tyne, UK

Shanmuganathan Gunalan

School of Engineering and Built Environment, Griffith University, Queensland, Australia

Perampalam Gatheeshgar

School of Computing, Engineering and Digital Technologies, Teesside University, UK

Konstantinos Daniel Tsavdaridis

School of Mathematics, Computer Science and Engineering, City, University of London, UK

Marco Corradi

Faculty of Engineering and Environment, Northumbria University, Newcastle upon Tyne, UK

Abstract:

Cold-Formed Steel (CFS) has been used to a great extent due to the industry uptake given its merits with the key being its high strength-to-weight ratio. Besides, innovative section profiles are constantly introduced to uplift the structural applicability of CFS sections. SupaCee section is a novel section with enhanced structural performance due to its sectional attributes such as longitudinal web stiffeners and return lips. However, the necessity of web openings (holes) to provide service integrations is not considered adequately so far in previous studies with SupaCee sections. Hence, this study reports a comprehensive assessment on flexural performance of SupaCee sections with web openings. Accordingly, numerical analysis was carried out which followed by the validation of the elaborated Finite Element (FE) model and the development of parametric studies considering key parameters such as depth, thickness, yield strength, web opening ratio and hole spacing. Results from the numerical studies are discussed and compared with existing design standards. New design provisions are proposed to predict the flexural capacity of SupaCee sections with web openings. Moreover, FE model of Lipped Channel Beam (LCB) was developed and analysed with similar parameters of SupaCee sections. The comparison of LCB and SupaCee sections with and without web openings are reported and based on the flexural capacity comparisons; recommendations are stated to replace conventional CFS sections by SupaCee sections.

Keywords: *Cold-formed steel; SupaCee section; Flexural performance; Web opening; Finite element modelling*

Nomenclature

d	Section depth	d_{wh}	Diameter of the hole
E	Modulus of elasticity	d_1	Clear web height
t	Thickness of the section	M_{ne}	Nominal member flexural strength for lateral torsional buckling
M	Ultimate bending capacity	M_{crl}	Critical elastic local buckling moment
f_y	Yield strength	λ_l	Non-dimensional slenderness value.
q_s	Reduction factor	M_{nd}	Nominal member moment capacity for distortional buckling
S	Hole spacing	M_y	Member yield moment
M_{nl}	Nominal member moment capacity at local buckling	M_{crd}	Critical elastic distortional buckling moment
M_p	Plastic moment	M_{ny}	Inelastic moment for extended slenderness limit;
C_{yd}	Distortional yield strain multiplier	C_{yl}	Local yield strain multiplier
M_{crlg}	Critical elastic local buckling moment at gross cross-section	M_{crlh}	critical local buckling moment of compressed section above the web opening
M_{crdg}	Critical elastic distortional buckling moment of gross cross-section	M_{crdn}	Critical elastic distortional buckling moment at a web opening
I_X	Second moment of area		

1 Introduction

Cold-Formed Steel (CFS) sections are being used as primary and secondary load-bearing members for over 100 years but have now been introduced into new areas of construction including modular construction [1] due to their merits and efficiencies such as light weight, high strength-to-weight ratio and flexibility. Meanwhile, highly optimised cross-section profiles of CFS sections have been emerged to improve their structural performance. Fig.1 shows the innovative cross-section profiles which were introduced in the CFS industry across various countries such as Australia, the United Kingdom and New Zealand. Subsequently, SupaCee sections were developed by BlueScope Lysaght and the University of Sydney to attain economical beneficiary as well as better structural performance [2]. Pham and Hancock [3] stated that SupaCee sections are performing well compared to conventional CFS channel sections in terms of bending capacity due to their longitudinal web stiffeners as well as return lip stiffeners. Consequently, SupaCee sections replaced general CFS sections in construction applications such as wall studs, roof systems and steel housing frames [3]. Since only a few research investigations in terms of structural performances of SupaCee sections have been carried out, applications of SupaCee sections are limited to some extent. Hence, this study reports the flexural performance of SupaCee sections with and without web openings, as the web openings are essential in a building to accommodate the services such as electrical, plumbing and heating [4]. Fig.2 illustrates the service integration through the web openings of beams in a typical building [5-6].

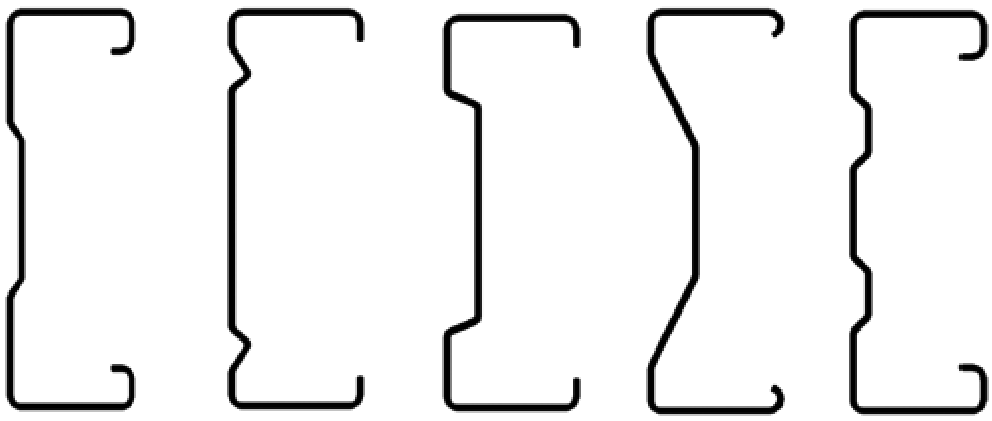

(a) (b) (c) (d) (e)

Fig.1: Cross section profiles : (a) DHS (Diamond Hi-Span); (b) Ultra BEAM; (c) Albion Sigma beam; (d) King span; (e) HST [2]

Experimental as well as numerical investigations were performed by many researchers to report the flexural behaviour of CFS sections. For example, Yu and Schafer [7] performed experimental distortional buckling tests on CFS sections (C- and Z-sections) under four-point bending to predict the section moment capacities in distortional buckling failure mode. Later, Yu and Schafer [8] performed an extensive numerical study of CFS sections after validating the numerical results against experimental values. Notably, numerical results indicated that existing Direct Strength Method (DSM) based equations were applicable to calculate the distortional and local buckling moments of CFS sections. Further numerical investigations were carried out to analyse the effect of distortional buckling under moment gradient, which was employed by applying the concentrated load at the mid span. An empirical equation was proposed to predict the distortional buckling moment with the influence of moment gradient. Subsequently, Yu and Yan [9] presented an Effective Width Method (EWM) to predict the distortional buckling strength of CFS sections (with C- and Z-profiles) under bending, which exhibited similar performance compared to DSM in terms of accuracy and reliability. Similarly, Kankanamge and Mahendran [10] proposed modified design equations to predict the lateral torsional buckling capacity of Lipped Channel Beam (LCB), whereas Anbarasu [11] presented a modified design equation to calculate elastic distortional buckling moment of LCB sections while the equation was valid only when both distortional and local buckling moments were nearly equal. Meanwhile, a Finite Element (FE) model was developed by Haidarali and Nethercot [12] to analyse the local buckling and combined distortional with local buckling behaviour of laterally restrained CFS sections.

Fig.2: Service integration through web openings [5-6]

Wang and Young [13] studied the flexural behaviour of CFS sections with stiffened webs and proposed modified DSM equations to predict the flexural capacities of CFS sections with stiffened cross-sections based on the obtained experimental and numerical results. Gatheeshgar et al. [14] investigated the elastic buckling behaviour and flexural performance of Modular

Construction Optimised (MCO) beams and proposed new DSM design equations to determine ultimate flexural capacities and elastic buckling moments of MCO beams. Flexural performance of high strength LCB sections and SupaCee sections was experimentally analysed by Pham and Hancock [3]. Twenty-four sections of two different section depths as well as three different thicknesses were considered for the experimental programme. Four-point experimental setup used by Pham and Hancock [3] is shown in Fig.3. The range of 4.5% - 22.4% flexural capacity enhancement in SupaCee sections compared to plain C sections was recorded by Pham and Hancock [3] and the reasons stated for the improved flexural capacity were longitudinal stiffeners and return lips which are featured in SupaCee sections. However, extensive numerical studies of flexural performance of SupaCee sections are not reported to till date.

Fig.3: Four-point bending experimental configuration [3]

Structural behaviour in terms of flexural [4, 15-21], shear [22-31], web crippling [32-41] and web-post buckling [42-43] of CFS sections with web openings is another area where research was conducted considering the web openings in beam sections to integrate electric and hydraulic services. Moen and Schafer [15] investigated the elastic buckling behaviour of CFS sections with web openings and proposed appropriate methods based on the DSM to determine their elastic buckling strengths. Later, Zhao et al. [16] reviewed the flexural performance of CFS sections with web openings and proposed modified formulas based on the DSM to predict their flexural capacities. Yu et al. [17] presented an analytical approach to determine the distortional buckling strength of CFS sections with circular web openings based on the

Hancock's [18] method which was proposed to calculate the distortional buckling stress of CFS sections without web openings subjected to pure bending. Chen et al. [4] conducted experimental and numerical analysis on LCB sections with web openings, stiffened web openings and plain webs in terms of flexural performance and compared the results with existing design standards as well as design equations which were proposed earlier by Moen and Schafer [15].

Flexural performance of SupaCee sections with web openings should had been analysed as it could display better structural performance compared to other CFS sections due to its cross-section profile. However, the flexural behaviour of SupaCee section with web openings is not explored up to date. In addition, extensive numerical analysis on SupaCee sections with respect to their flexural behaviour is not reported. Hence, this study aims to enhance the applicability of SupaCee sections in the industry by studying their flexural behaviour with openings. Comprehensive numerical studies of flexural behaviour of SupaCee sections with and without the unstiffened web openings is conducted and modified equations with reduction factors are provided to predict the ultimate flexural capacity of SupaCee section with web openings. Moreover, ultimate flexural capacities of SupaCee sections are compared with similar LCB sections and recommendations are stated to replace conventional CFS sections by SupaCee sections with web openings.

2 Numerical Investigation

2.1 Overview

The numerical models were developed simulating the actual experimental setup of four-point bending case with the FEA software, ABAQUS [44]. Moreover, developed FE model consists SupaCee section as well as Web Side Plates (WSP). SupaCee sections with and without web openings were modelled using the middle surface offset definition which create the centreline of the section first and then generate the half of the thickness both side of the centreline dimension when applying the section assignments. Therefore, cross-section of the SupaCee section was generated using centre line to generate the actual sections. Besides, relevant material properties such as yield strength, density, Poisson's ratio and elastic modulus were added to the sections. Later, WSPs were assembled to the SupaCee section according to the four-point bending setup using 'tie' constraint which ties beam and WSPs together. Assembly of WSPs to the SupaCee section by using the surface-to-surface 'tie' constraint is illustrated in

Fig.4. Master and slave surfaces were chosen during the tie constraint application also mentioned in Fig.4.

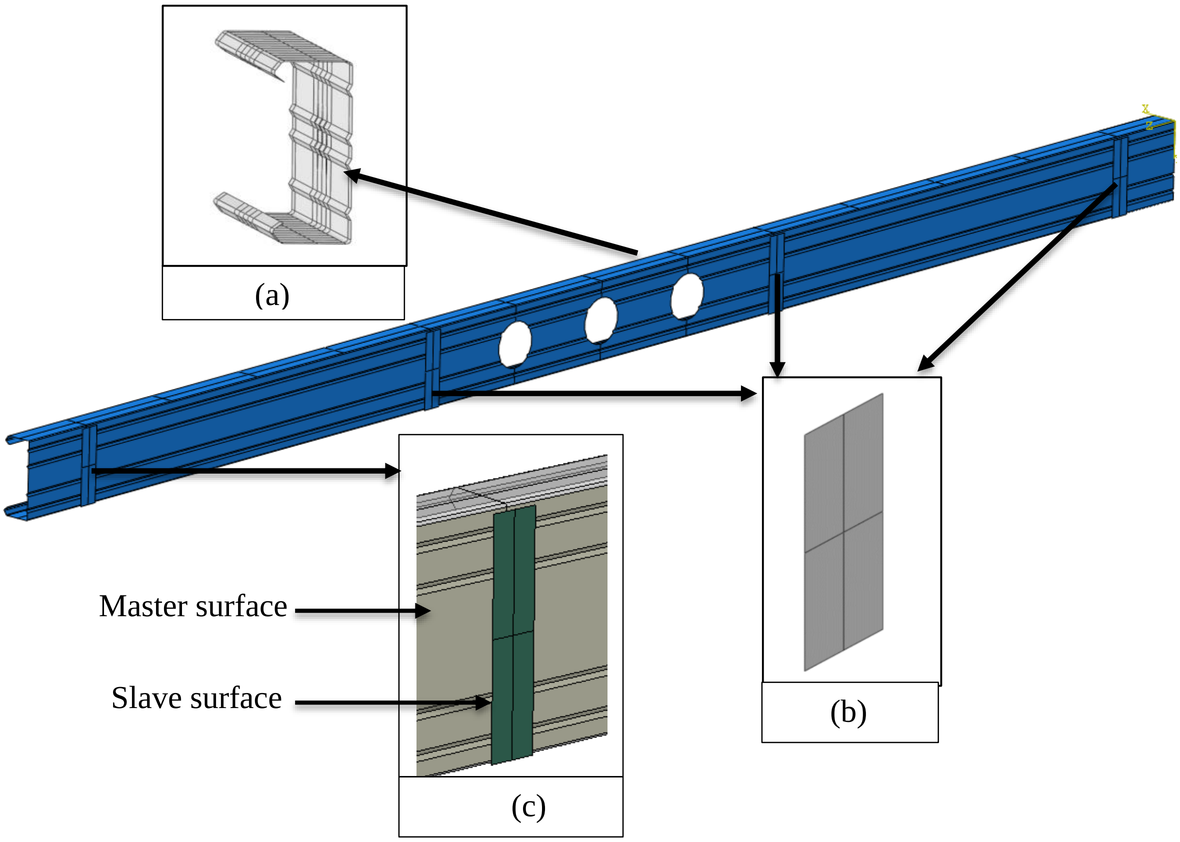

Fig.4: Surface to surface assembly of SupaCee beam and WSP: (a) SupaCee beam (b) WSP and (c) Master and slave surfaces in tie constraint

The simulation was carried out in two parts: Elastic buckling analysis to attain the eigen modes of the section and non-linear analysis to obtain the failure modes and the ultimate bending capacity. Buckling modes from the former analysis was used to add the initial geometric imperfection while performing non-linear analysis to stimulate the out-of-plane deformations of the section elements. Imperfection magnitude of 0.15t where t is the thickness of the section, was used in the numerical simulations as it was recommended by Pham and Hancock [45]. Comparison of obtained numerical results against experimental outcomes was stated by Pham and Hancock [45]. The comparison was done by changing the imperfection magnitudes as well as corresponding eigen modes and 0.15t imperfection magnitude was found appropriate for accurate replication of experimental condition. The static general analysis was employed with non-linear analysis after taking in to the consideration of validation procedure and previous similar work [46]. A comprehensive description regarding the numerical analysis of flexural behaviour of the SupaCee sections with openings is provided next.

2.2 Element type and meshing scheme

S4R shell element type was opted to model the SupaCee section as its thickness was negligible compared to other dimensions, whereas R3D4 rigid element was selected for WSP to represent the rigid nature of WSP. Similar several research studies [36-39, 46] employed S4R element type due to its merits such as accuracy, reduced integration and lesser-required time. Hence, four-node S4R shell element was preferred over other shell element types available in ABAQUS.

Meshing scheme was selected by considering similar research studies [36-39, 46] and the results from the mesh sensitivity analysis. 5 mm x 5 mm mesh size was provided to SupaCee section with and without openings. However, Corner regions of the section were refined by finer mesh size of 1 mm x 5 mm to neglect the effects on ultimate strength due to the curvature of the section. Similar concept was considered by Perera and Mahendran [47] in the corner sections. Subsequently, coarse mesh size of 10 mm x 10 mm was selected for the WSP. In addition, mesh control with medial axis algorithm was applied to ensure the smooth mesh pattern near web openings. Provided meshing scheme for the FE model is illustrated in Fig.5.

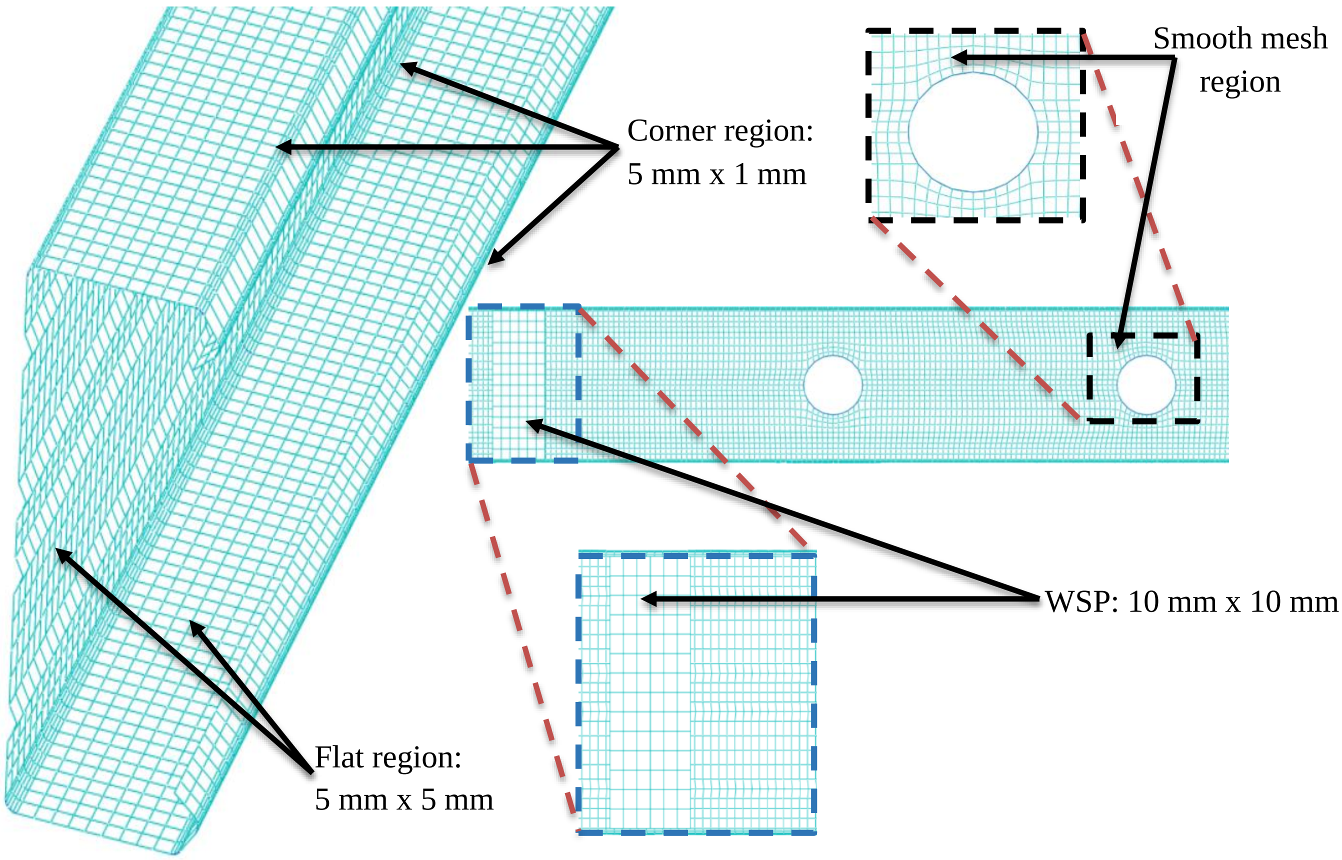

Fig.5: Mesh scheme of the numerical study

2.3 Material model

Selection of material characteristics of SupaCee section is significant in the numerical analysis considering the accuracy of the obtained ultimate bending capacities and failure modes. Stress-strain behaviour of CFS was used in the numerical modelling with negligible strain hardening based on the past studies [36-39, 48]. Besides, elastic perfectly plastic material model with nominal yield strength was employed. Corner strength enhancement and residual stress were neglected in the analysis as they compensate each other [49]. SupaCee section was modelled with the density, elastic modulus and Poisson's ratio values of 7850 kg/m^3, 200 GPa and 0.3, respectively.

2.4 Boundary condition and load application

Four-point bending setup was selected for the numerical analysis to ensure the failure is purely bending at the mid-span where the ultimate bending capacities would be obtained. Reference points were added in the WSPs to assign the load and boundary conditions. Simply supported boundary conditions and loading conditions were employed at the reference points of WSPs using displacement control method. Moreover, lateral restraints were added in the SupaCee section at the centre of top and bottom flanges in 300 mm intervals to eliminate lateral torsional and distortional buckling and to ensure the local buckling failure in the beam. Fig.6 depicts the assigned boundary conditions and loading application of the SupaCee section. Load application properties such as maximum load increments (1000), initial increment size (0.01), total time period (1.0), minimum increment size (1×10^{-25}) and maximum increment size (0.1) were selected based on the previous numerical studies [36-39].

3 Validation and Parametric plan

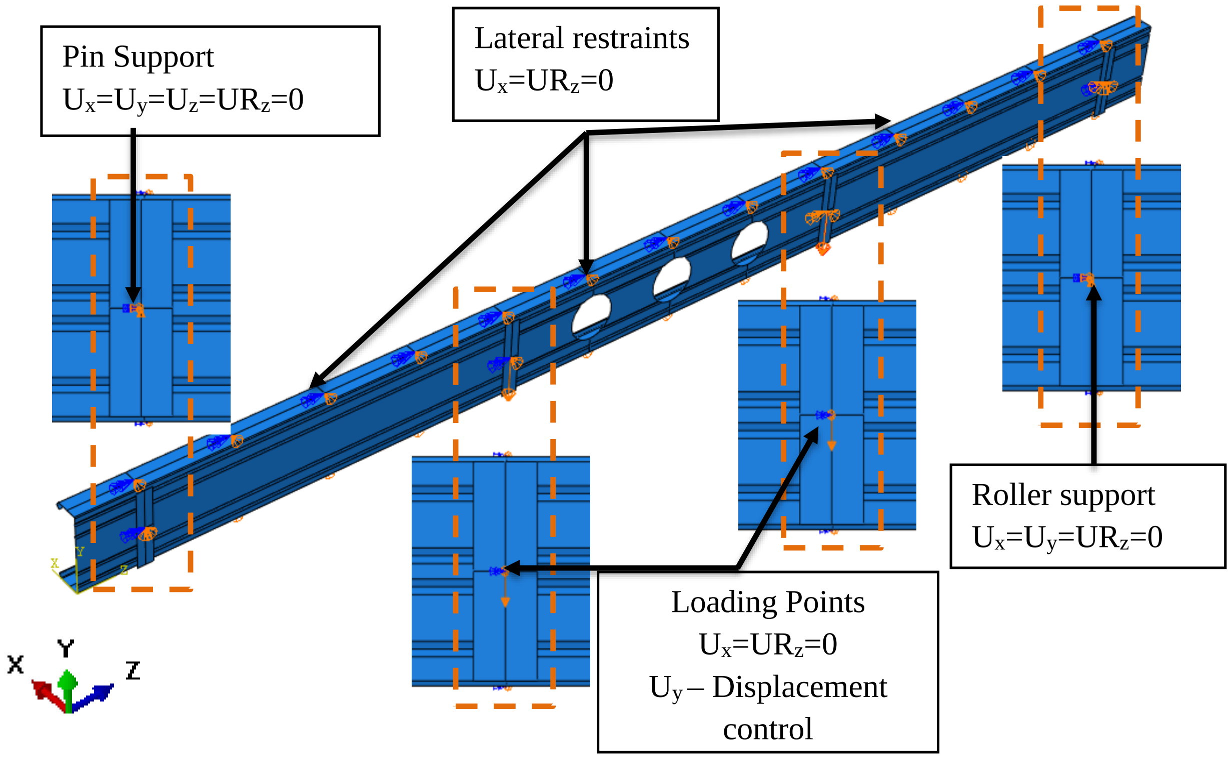

Fig.6: Applied boundary conditions and loading terms

3.1 Validation of FE model

Validation is mandatory before numerical analysis as it is important to ensure the reliability of the results from the parametric study. Hence, through the validation procedure, selected modelling features including element types, meshing scheme, material properties, boundary conditions, imperfections and non-linear analysis method can be justified. Experimental results from the Pham and Hancock's study [3] on SupaCee sections were taken for the validation of the numerical analysis which investigates the flexural behaviour of SupaCee section with web openings. Pham and Hancock [3] conducted experiments on SupaCee section with two different section depths (150 mm and 200 mm) and three different thicknesses (1.2 mm, 1.5 mm and 2.4 mm). Altogether six experimental results were taken in-to consideration for the validation and Table 1 shows validation results and the comparison between FEA and experimental results.

Table 1: Comparison of FE results against experimental results

Section	Sectional depth (d)	Thickness of section (t)	Material yield strength (f_y)	Experiment results [3]	FEA values	Experiment/FEA
	(mm)	(mm)	(MPa)	(kNm)	(kNm)	
SC15012	150	1.2	589.71	8.19	7.97	1.03
SC15015	150	1.5	533.88	11.40	9.98	1.14
SC15024	150	2.4	513.68	21.19	19.91	1.06
SC20012	200	1.2	593.30	10.71	10.04	1.07
SC20015	200	1.5	532.03	16.48	14.89	1.11
SC20024	200	2.4	504.99	33.82	29.79	1.14
Mean						1.09
COV						0.04

Obtained FEA results against experimental results shown good agreement with the mean value of 1.09 and Coefficient of Variation (COV) value of 0.04. Subsequently, failure mode and load vs deflection curve of the experimental section and FE model were compared. Results of both comparisons are illustrated in Fig.7 and Fig.8, respectively. Both Comparisons reported a good resemblance between FE model and the experimental setup.

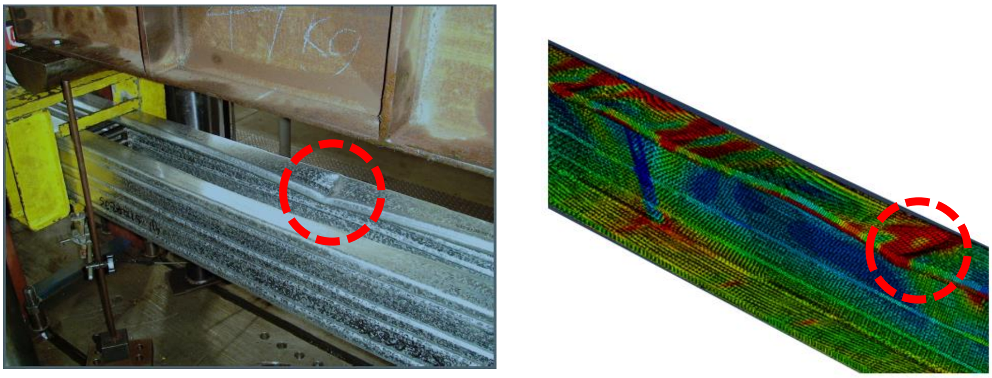

(a) Experimental Set-up [3]

(b) FEA

Fig.7: Failure pattern comparison for SC20015 [3]

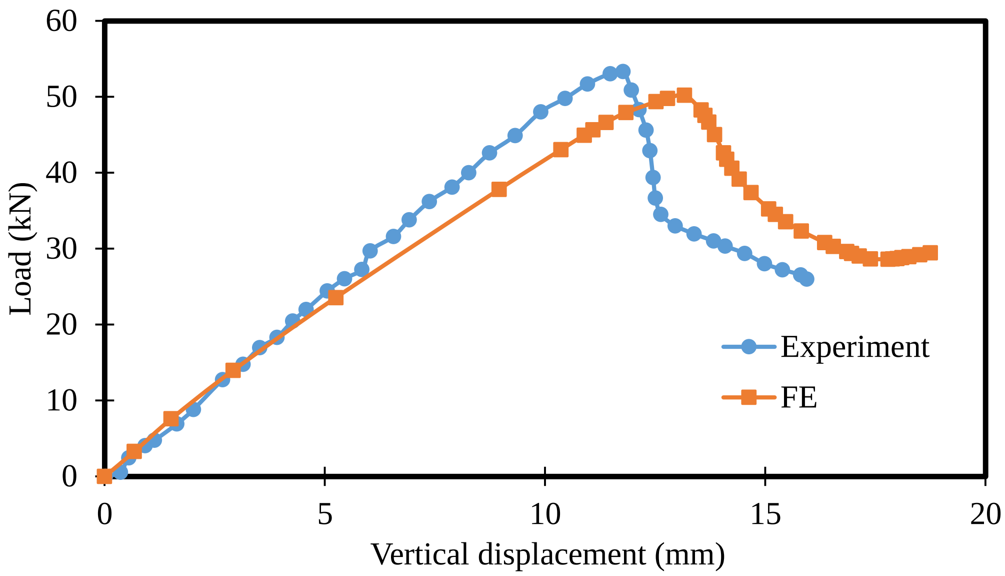

Fig. 8: Load vs. deflection curve for section SC20012 [3]

Similarly, validation procedure was conducted to verify the FE models with web openings against experimental results. Research work from Chen et al. [4] in the flexural behaviour of CFS sections (Lipped Channel Beam (LCB)) with and without web openings was taken for the validation purpose. Validation results are stated in Table 2 and the comparison indicated good agreement between FEA and test results with the mean value of 0.95 and COV value of 0.05. Fig.9 and Fig.10 illustrates the failure mode and load vs. deflection curve comparisons which also showed a good agreement of the FE results. Since developed models using ABAQUS predicted the flexural behaviour of SupaCee sections without openings and LCB sections accurately, the developed numerical model was taken in to consideration for the parametric studies. This numerical approach ensures the effect of web stiffeners and return lips by validating the SupaCee section without web openings and effect of web openings by validating LCB sections. Besides, the similar numerical combination approach was followed in similar studies earlier [31]. Hence, based on the validation process, results and comparisons, developed numerical model was selected to carry out the parametric study and to analyse the flexural behaviour of SupaCee sections with web openings.

Table 2: Comparison of section moment capacity between FE results and test [4]

Specimen	Hole diameter (mm)	Hole spacing (mm)	Test [4] (kNm)	FE (kNm)	Test/FE
Plain section					
240-L4000-NH	–	–	11.90	11.63	1.02
290-L4000-NH	–	–	18.00	19.15	0.94
Un-stiffened web openings					
240-L4000-UH1	141.5	–	11.00	11.25	0.98
240-L4000-UH3	140.8	100	10.60	11.20	0.95
290-L4000-UH1	141.5	–	16.70	18.74	0.89
290-L4000-UH3	141.9	100	16.30	17.90	0.91
Mean					0.95
COV					0.05

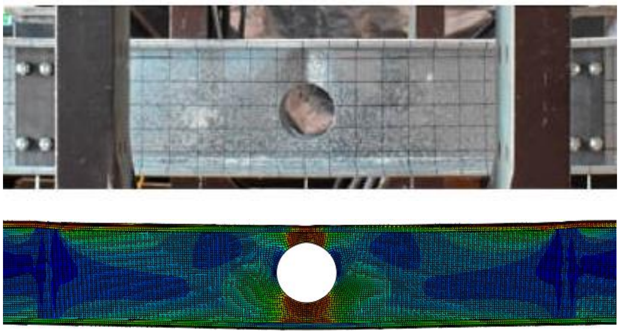

(a)

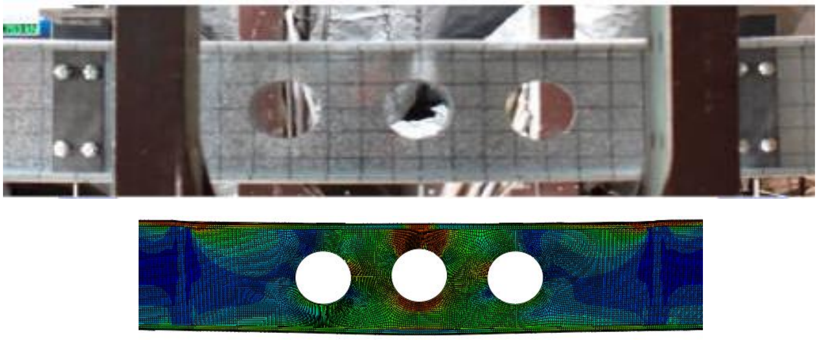

(b)

Fig.9: Failure Pattern Comparison of section: (a) 240-L4000-UH1; (b) 290-L4000-UH3 [4]

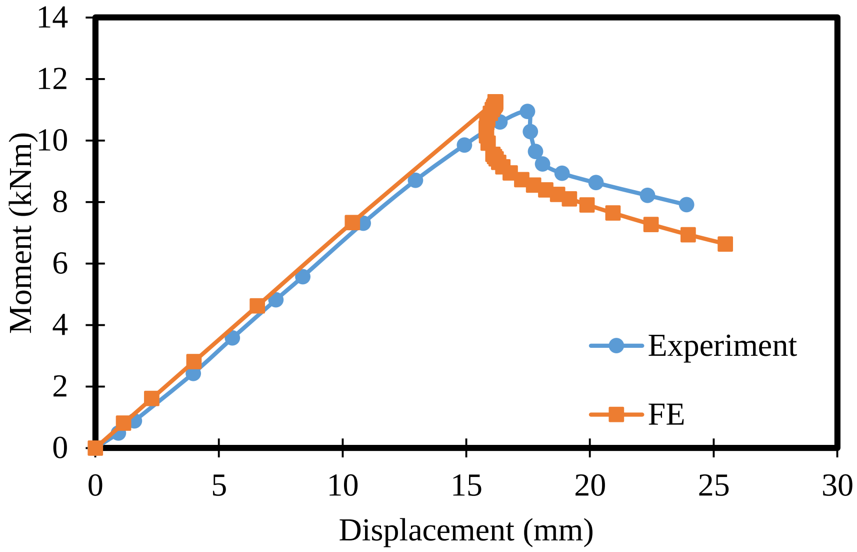

(a)

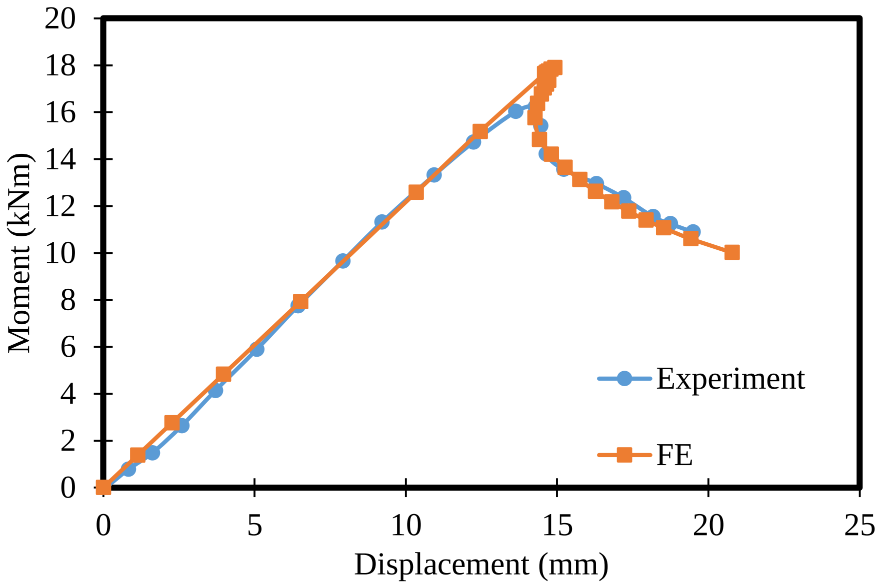

(b)

Fig.10: Comparison of moment vs. displacement curve for sections: (a) 240-L4000-UH1 and (b) 290-L4000-UH3

3.2 Parametric plan

Parametric plan to carry out an extensive study on the flexural performance of SupaCee sections with web openings was developed based on the critical parameters after the validation process of numerical models. Accordingly, three various section depths (150 mm, 200 mm and 250 mm) and three different thicknesses (1 mm, 2 mm and 2.5 mm) were selected as the key dimensions of the SupaCee section. Parametric dimensions of the SupaCee section are provided in Fig.11 and Table 3.

Web opening ratios (d_{wh}/d_1) were selected as 0.0, 0.4, 0.6 and 0.8 and material yield strengths were considered as 300 MPa, 450 MPa and 600 MPa. Industrial requirements and previous studies [27, 36, 38, 48] were considered to select the web opening sizes and stress-strain behaviour was opted based on elastic perfectly plastic model as described earlier. In addition, effect of spacing between web openings was considered in this study. Hence, two different spacing (300 mm and 450 mm) were planned to provide between the web openings which dimension considered between web opening centres. Parametric plan was drafted considering all afore mentioned parameters and provided in Table 4. Overall, 189 FE models were planned to analyse the flexural performance of SupaCee section with and without web openings in this study.

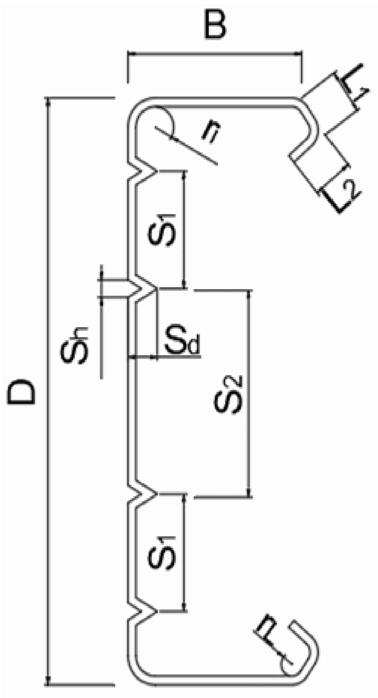

Fig. 11: Cross-section profile of SupaCee beam

Table 3: Selected dimensions of SupaCee section

H (mm)	B (mm)	L_1 & L_2 (mm)	a_1 (mm)	a_2 (mm)	S_1 (mm)	S_2 (mm)	S_h (mm)	S_d (mm)	r_i & r_l (mm)
150	50	12	125	95	40	20	10	5	2
200	65	15	125	95	40	70	10	5	2
250	75	15	125	95	40	120	10	5	2

Table 4: Parametric plan

Section	Thickness	web hole diameter ratio	Hole spacing	Strength	No. of Models
H x B (mm x mm)	t (mm)	d_{wh}/d_1	S (mm)	f_y (MPa)	
Plain section					
150 × 50	1, 2, 2.5	0	-	300, 450, 600	9
200 × 65	1, 2, 2.5	0	-	300, 450, 600	9
250 × 75	1, 2, 2.5	0	-	300, 450, 600	9
Un-stiffened web openings					
150 × 50	1, 2, 2.5	0.4, 0.6, 0.8	300, 450	300, 450, 600	54
200 × 65	1, 2, 2.5	0.4, 0.6, 0.8	300, 450	300, 450, 600	54
250 × 75	1, 2, 2.5	0.4, 0.6, 0.8	300, 450	300, 450, 600	54
Total					189

4 Results and Discussion

Detailed numerical analysis was carried out based on the results from the comprehensive parametric study are provided and discussed in this chapter. Table.5 outlines the obtained ultimate bending capacities (M) with corresponding web opening ratios (d_{wh}/d_1), hole spacing (S), thickness (t) and yield strengths (f_y).

Table.5: Parametric study results

H	t	d_{wh}/d_1	S = 300 mm			S = 450 mm		
			f_y = 300 MPa	f_y = 450 MPa	f_y = 600 MPa	f_y = 300 MPa	f_y = 450 MPa	f_y = 600 MPa
(mm)	(mm)		M (kNm)	M (kNm)	M (kNm)	M (kNm)	M (kNm)	M (kNm)
150	1	0	4.12	5.89	7.23	4.12	5.89	7.23
150	1	0.4	2.95	4.48	5.73	2.88	4.42	5.29
150	1	0.6	2.83	4.26	5.30	2.52	3.91	5.11
150	1	0.8	1.95	2.93	3.65	1.38	2.36	3.10
150	2	0	9.05	13.05	17.07	9.05	13.05	17.07
150	2	0.4	7.00	11.41	15.15	6.89	11.09	14.78
150	2	0.6	6.78	10.84	14.46	6.25	10.27	14.02
150	2	0.8	4.88	7.95	10.82	4.08	7.08	10.01
150	2.5	0	10.01	16.04	22.15	10.01	16.04	22.15
150	2.5	0.4	8.69	14.38	19.79	8.58	13.87	18.66
150	2.5	0.6	8.36	13.57	18.13	7.76	12.74	17.63
150	2.5	0.8	6.15	10.00	13.71	5.17	8.93	12.64
200	1	0	6.04	9.11	9.54	6.04	9.11	9.54
200	1	0.4	4.14	5.88	6.93	4.05	5.83	6.41

200	1	0.6	4.05	5.77	5.89	3.54	5.13	5.37
200	1	0.8	3.21	4.53	5.56	2.63	3.94	4.96
200	2	0	12.98	21.89	29.02	12.98	21.89	29.02
200	2	0.4	10.80	17.05	21.25	10.70	16.38	21.17
200	2	0.6	10.56	16.80	20.60	9.64	15.26	20.00
200	2	0.8	8.68	13.56	17.26	7.55	12.18	16.41
200	2.5	0	17.05	27.05	35.89	17.05	27.05	35.89
200	2.5	0.4	13.69	21.57	28.57	13.46	21.07	27.91
200	2.5	0.6	12.98	21.03	27.58	12.03	19.30	26.03
200	2.5	0.8	11.02	17.02	23.41	9.72	16.02	21.91
250	1	0	9.55	11.11	13.44	9.55	11.11	13.44
250	1	0.4	7.01	9.55	11.39	6.99	9.57	11.34
250	1	0.6	6.90	8.98	10.44	6.24	8.47	10.30
250	1	0.8	5.81	7.85	9.48	5.14	7.36	9.16
250	2	0	19.05	28.85	38.20	19.05	28.85	38.20
250	2	0.4	18.57	27.92	35.22	18.33	27.85	34.73
250	2	0.6	18.09	26.77	32.46	16.61	25.07	31.93
250	2	0.8	15.13	22.73	28.88	13.74	20.87	27.15
250	2.5	0	26.08	38.40	54.02	26.08	38.40	54.02
250	2.5	0.4	24.63	37.08	51.46	24.12	36.89	48.23
250	2.5	0.6	23.85	35.31	45.46	21.34	33.87	43.49
250	2.5	0.8	19.45	30.10	39.92	17.50	28.34	37.93

Fig.12 illustrates the failure modes of section 150×50×1 ($d_{wh}/d_1 = 0.4$) at various stages with load-deflection curve obtained from the numerical analysis. Moreover, initial imperfection contour of the same section is illustrated in Fig.12. Meanwhile, Fig.13 compares the load-deflection curve of section 150×50×2 ($d_{wh}/d_1 = 0.4$) with hole spacing (300 mm and 450 mm). Based on the results, it can be stated that hole spacing has little impact on the ultimate bending capacity of SupaCee sections with web openings and the results indicated that lesser space between web openings is beneficial in terms of flexural capacity.

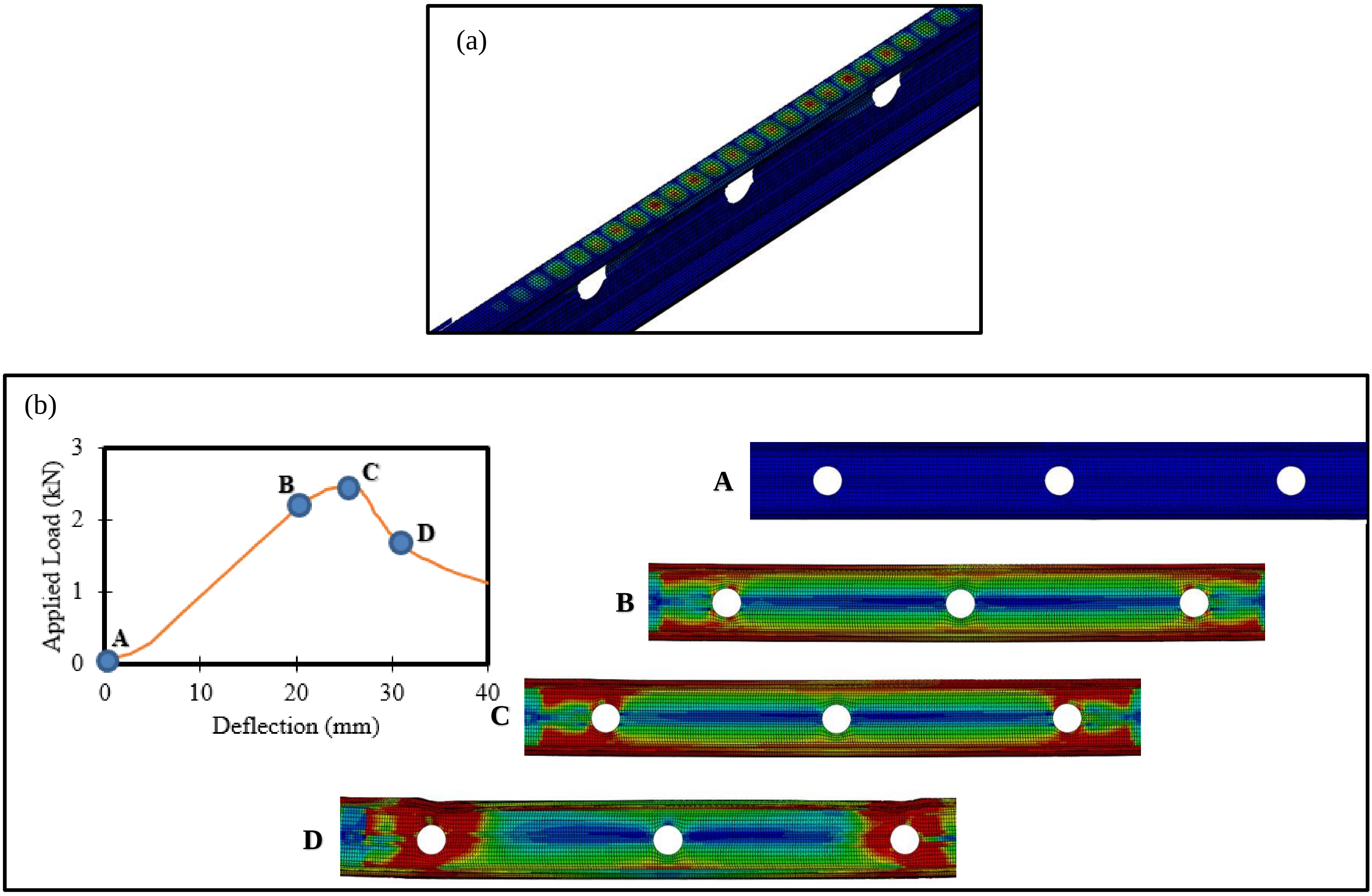

Fig.12: (a) Initial imperfection contours and (b) failure modes of section 150x50x1 ($d_{wh}/d_1 = 0.4$)

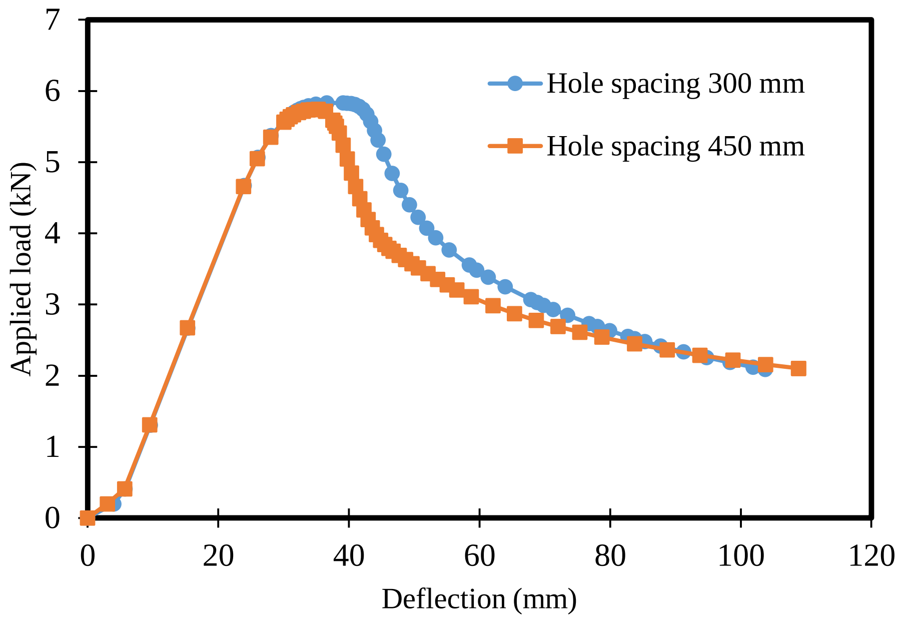

Fig.13: Load vs deflection curve comparison (150×50×2) with hole spacing

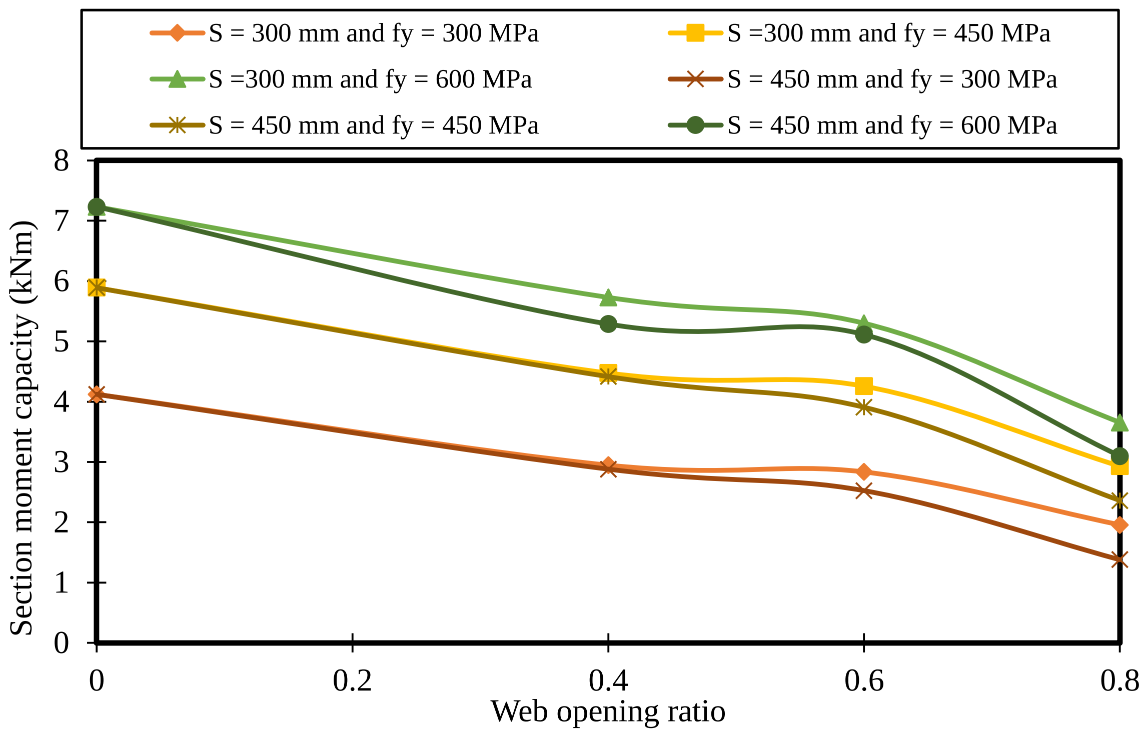

Fig.14: Comparison of flexural capacities with hole spacing (S) and yield strength (f_y) for 150 mm section (t = 1 mm)

Fig.15 shows flexural capacity variation with respect to thickness of different sections with web openings. Comparison indicates that increase in thickness will improve the flexural capacity of SupaCee section. Similarly, Fig.16 demonstrates the impact of yield strength in flexural capacity of SupaCee sections with web openings and high yield strength section shows improved bending capacity. Moreover, Fig.17 compares the load vs. deflection curve obtained of the 200 mm section for different web opening ratios, where a sudden drop is evident in web opening ratio of 0.8. Reduction area in web stiffeners due to web openings is lesser in web opening ratios of 0.4 and 0.6, whereas in web opening ratio of 0.8 reduction area is higher as it cut through all four web stiffeners in the SupaCee section. Hence, a significant decline is observed in between web opening ratio of 0.6 to 0.8. Fig.18 displays the failure patterns for the corresponding sections respectively.

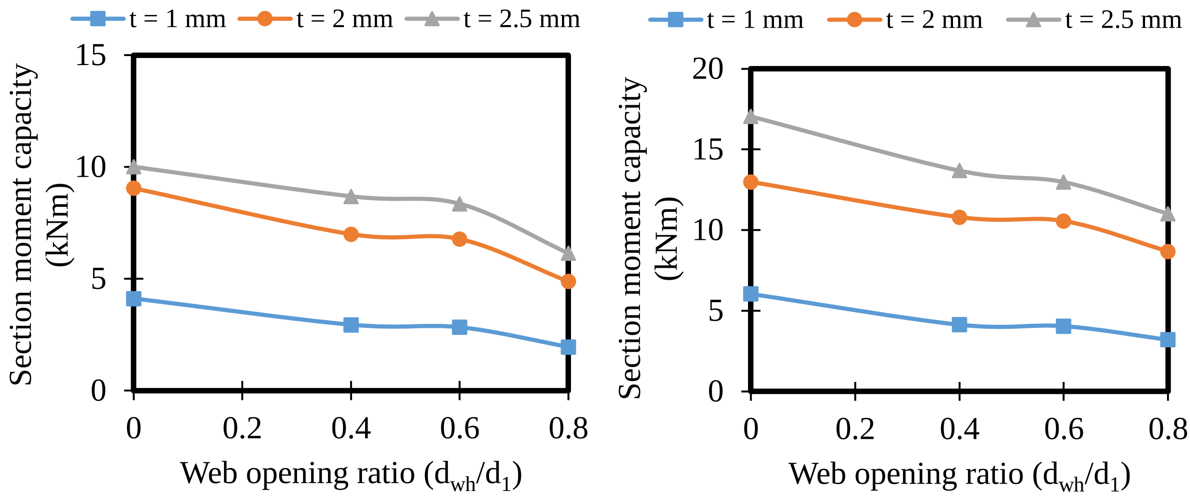

(a) Section 150 (b) Section 200

Fig.15: Comparison of flexural capacities with thickness (f_y = 300 MPa)

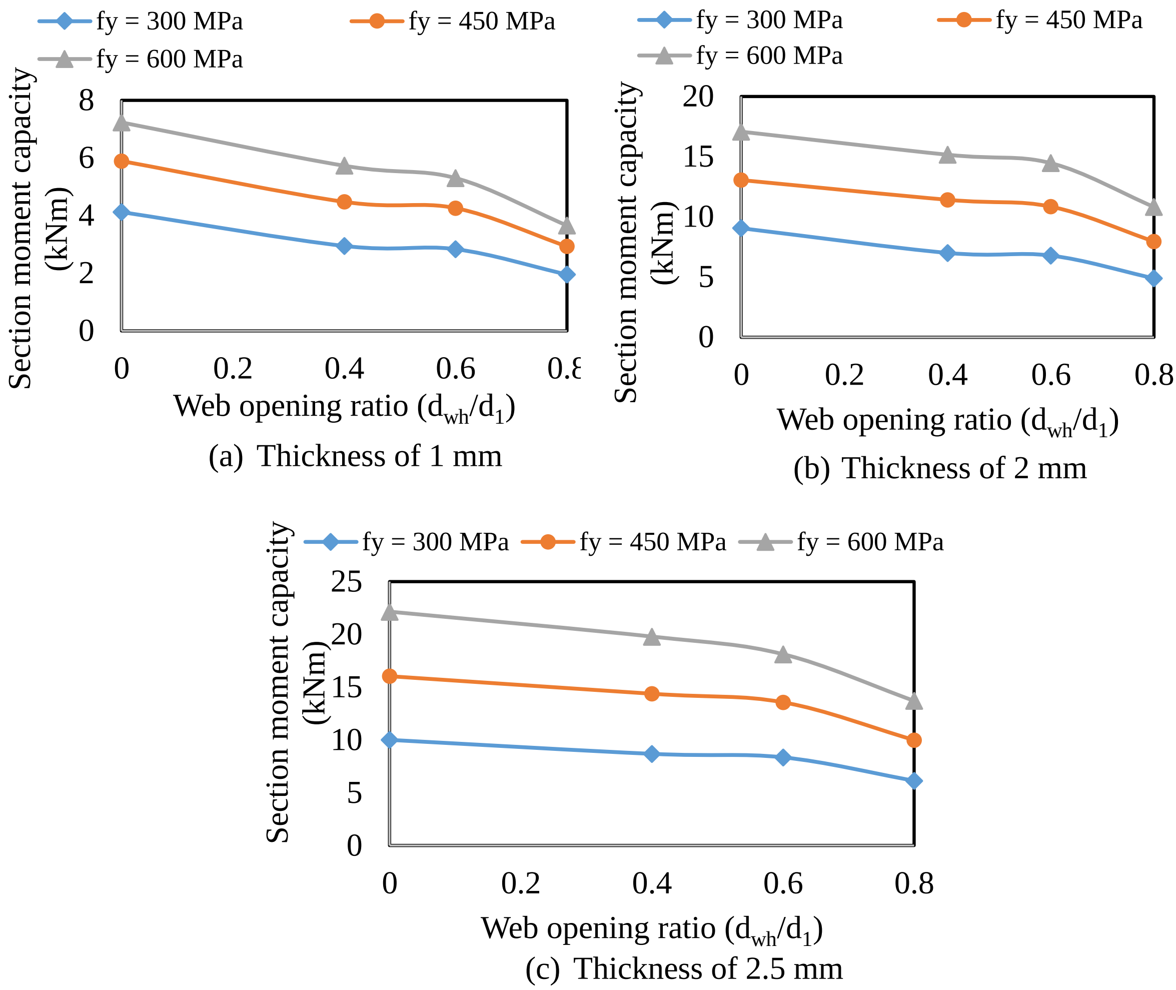

Fig.16: Comparison of flexural capacities with yield strength (Section 150)

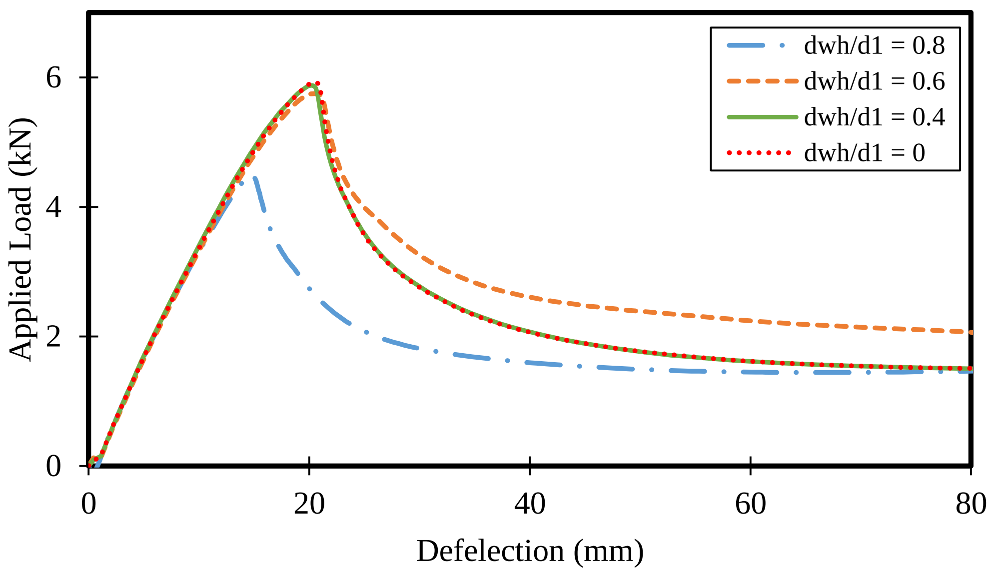

Fig.17: Load vs. deflection curve comparison with web opening ratio

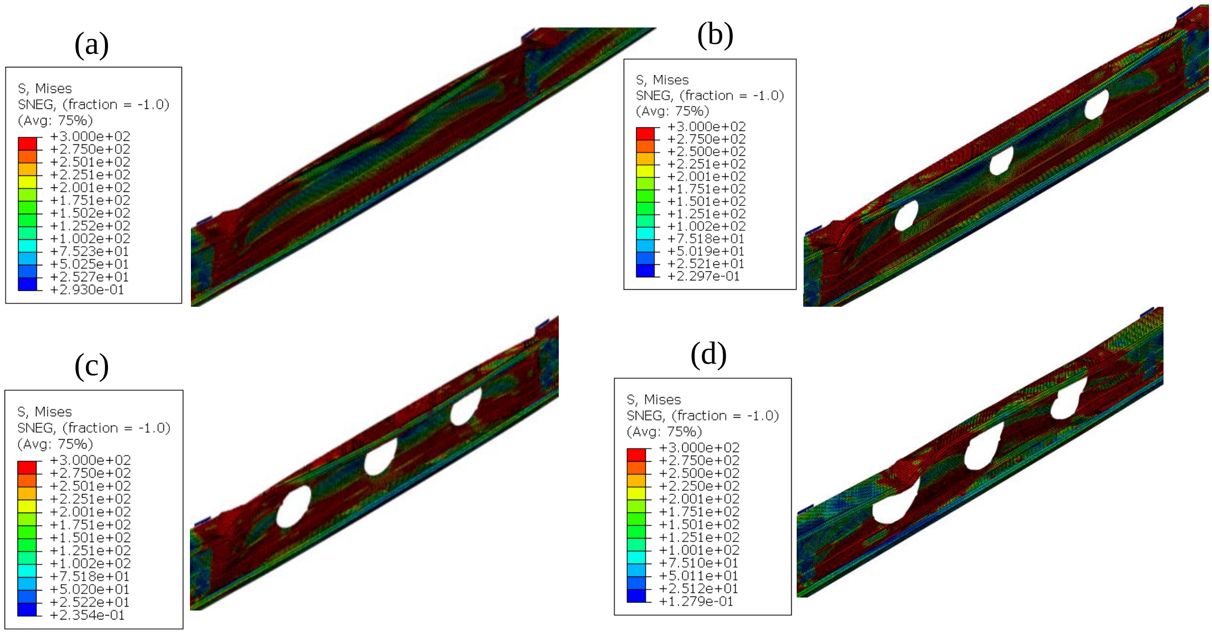

Fig.18: Failure mode comparison with various web opening ratio: (a) $d_{wh}/d_1 = 0$; (b) $d_{wh}/d_1 = 0.4$; (c) $d_{wh}/d_1 = 0.6$; (d) $d_{wh}/d_1 = 0.8$

5 Current design rules for flexural behaviour

This section reviews the existing design equations in previous research works on CFS sections as well as design standards such as AISI S100 [50] and AS/NZS 4600 [51] to calculate the flexural capacity of CFS sections without web openings and the proposed design formulas in the literature [3, 15-16] for section moment capacity of CFS sections with web openings.

AISI S100 [50] and AS/NZS 4600 [51] provide the following equations (Eqs. (1) – (3)) to predict the nominal moment capacity (M_{nl}) of CFS sections at local buckling.

$$M_{nl} = M_{ne} \qquad \text{for } \lambda_l \le 0.776 \tag{1}$$

$$M_{nl} = \left[1 - 0.15\left(\frac{M_{crl}}{M_{ne}}\right)^{0.4}\right]\left(\frac{M_{crl}}{M_{ne}}\right)^{0.4} M_{ne} \qquad \text{for } \lambda_l > 0.776 \tag{2}$$

$$\lambda_l = \sqrt{\frac{M_{ne}}{M_{crl}}} \tag{3}$$

Where, M_{nl} - nominal member moment capacity at local buckling; M_{ne} - nominal member flexural strength for lateral torsional buckling; M_{crl} - critical elastic buckling moment; λ_l- non-dimensional slenderness value for local buckling.

Eqs. (4) – (6) from AISI S100 [50] and AS/NZS 4600 [51] can be used to calculate the nominal moment capacity (M_{nd}) of CFS sections at distortional buckling.

$$M_{nd} = M_y \qquad \text{for } \lambda_d \leq 0.673 \tag{4}$$

$$M_{nd} = \left[1 - 0.22\left(\frac{M_{crd}}{M_y}\right)^{0.5}\right]\left(\frac{M_{crd}}{M_y}\right)^{0.5} M_y \qquad \text{for } \lambda_d > 0.673 \tag{5}$$

$$\lambda_d = \sqrt{\frac{M_y}{M_{crd}}} \tag{6}$$

Where, M_{nd} - nominal member moment capacity for distortional buckling; M_y - member yield moment ($M_y = S_f \times f_y$, S_f - section modulus; f_y - elastic distortional buckling stress); M_{crd} - critical elastic distortional buckling moment; λ_d- non-dimensional slenderness value for distortional buckling.

Shifferaw and Schafer [52] provided a general method to address the inelastic bending capacity of CFS sections based on the experimental and numerical data. The relationship of inelastic local buckling and lateral torsional buckling is provided by Eqs. (7) – (11) which were verified by Shifferaw and Schafer [52]. Later, Pham and Hancock [3] proposed equation (Eq. (12)) to predict inelastic local buckling and distortional buckling for extended slender sections. Moreover, Pham and Hancock [3] reported that existing design equations to predict the flexural capacities of CFS sections can be also applicable to SupaCee sections.

$$M_n = M_y + \left(1 - \frac{1}{C_y^2}\right)(M_p - M_y) \qquad \text{for} \quad \lambda_d \leq 0.673, \quad \lambda_l \leq 0.776 \tag{7}$$

$$\lambda_d = \sqrt{\frac{M_y}{M_{crd}}} \tag{8}$$

$$\lambda_l = \sqrt{\frac{M_y}{M_{crl}}} \tag{9}$$

$$C_{yd} = \sqrt{\frac{0.673}{\lambda_d}} \leq 3 \tag{10}$$

$$C_{yl} = \sqrt{\frac{0.776}{\lambda_l}} \leq 3 \tag{11}$$

$$M_{ny} = M_y + (1 - \tfrac{1}{C_y^2})(M_p - M_y) \qquad \text{for} \quad \lambda_{\mathrm{d}} \leq 1.45, \quad \lambda_l \leq 1.55 \tag{12}$$

Where, λ_l and λ_d – non-dimensional slenderness values; M_y – yield moment; M_p – plastic moment; M_{ny} – inelastic moment for extended slenderness limit; C_{yl} - local yield strain multiplier; C_{yd} – distortional yield strain multiplier

Moen and Schafer [15] investigated the flexural behaviour of CFS sections with web openings and proposed design equations to predict ultimate flexural strength based on the DSM which includes the influence of web openings. The equations were proposed for limit states including local and distortional buckling. The nominal flexural capacity for local buckling (M_{nl}) of CFS sections with unstiffened web openings can be calculated using Eqs. (13) – (16).

$$M_{nl} = M_{ne} \leq M_{ynet} \qquad \text{for } \lambda_l \leq 0.776 \tag{13}$$

$$M_{nl} = \left[1 - 0.15\left(\frac{M_{crl}}{M_{ne}}\right)^{0.4}\right]\left(\frac{M_{crl}}{M_{ne}}\right)^{0.4} M_{ne} \ \leq \ M_{ynet} \qquad \text{for } \lambda_l > 0.776 \tag{14}$$

$$\lambda_l = \sqrt{\frac{M_{ne}}{M_{crl}}} \tag{15}$$

$$M_{crl} = \min(M_{crlg}, M_{crlh}) \tag{16}$$

Where, M_{ni} - nominal flexural capacity of local buckling; M_{ynet}- member yield moment capacity of net cross-section; M_{crl} - critical elastic local moment (considering the influence of web openings); M_{ne}- nominal section moment capacity for lateral torsional buckling; M_{crlg}- critical elastic buckling moment at gross cross-section; M_{crlh}- critical local buckling moment of compressed section above the web opening; λ_l- non-dimensional slenderness value for local buckling.

DSM based design equations (Eqs. (17) - (24)) to calculate the nominal moment capacity for distortional buckling of CFS sections with web openings were proposed by Moen and Schafer [15].

$$M_{nd} = M_{ynet} \quad \text{for } \lambda_d \leq \lambda_{d1} \tag{17}$$

$$M_{nd} = M_{ynet} - \left(\frac{M_{ynet} - M_{d2}}{\lambda_{d2} - \lambda_{d1}}\right)(\lambda_d - \lambda_{d1}) \quad \text{for } \lambda_{d1} < \lambda_d \leq \lambda_{d2} \tag{18}$$

$$M_{nd} = \left[1 - 0.22\left(\frac{M_{crd}}{M_y}\right)^{0.5}\right]\left(\frac{M_{crd}}{M_y}\right)^{0.5} M_y \quad \text{for } \lambda_d > \lambda_{d2} \tag{19}$$

$$\lambda_d = \sqrt{\frac{M_y}{M_{crd}}} \tag{20}$$

$$\lambda_{d1} = 0.673\left(\frac{M_{ynet}}{M_y}\right)^3 \tag{21}$$

$$\lambda_{d2} = 0.673\left[1.7\left(\frac{M_y}{M_{ynet}}\right)^{2.7} - 0.7\right] \tag{22}$$

$$M_{d2} = \left(1 - 0.22\left(\frac{1}{\lambda_{d2}}\right)\right)\left(\frac{1}{\lambda_{d2}}\right) M_y \tag{23}$$

$$M_{crd} = \min(M_{crdg}, M_{crdn}) \tag{24}$$

Where, M_{nd} – section moment capacity for distortional buckling; M_{ynet}- member yield moment of net cross-section; M_{crd}- critical elastic distortional buckling moment (including the effect of web openings); M_{crdg}- critical elastic distortional buckling moment of gross cross-section; M_{crdn}- critical elastic distortional buckling moment at a web opening; M_y- member yield moment; λ_{d1}, λ_d and λ_{d2} - non-dimensional slenderness values.

Zhao et al. [16] modified existing design equations to predict the flexural capacity of CFS sections with web openings as it was found that web openings were influencing failure modes by changing the failure modes from only local buckling or only distortional buckling to local-distortional buckling interaction controlled by local buckling or distortional-local buckling interaction controlled by distortional buckling. Hence, Zhao et al. [16] proposed modified design equations (Eqs. (25) – (30)) based on the numerical results to predict the nominal flexural strength of CFS section with web openings controlled by distortional buckling. Similarly, Eqs. (31) – (35) were proposed to predict the flexural capacity of CFS sections with web openings controlled by local buckling according to Zhao et al. [16].

$$M_{nd} = M_{ynet} \qquad \text{for } \lambda_d \leq \lambda_{d1} \tag{25}$$

$$M_{nd} = M_{ynet} - \left(\frac{M_{ynet} - M_{d2}}{\lambda_{d2} - \lambda_{d1}}\right)(\lambda_d - \lambda_{d1}) \leq 0.88\left[1 - 0.2\left(\frac{M_{crd}}{M_y}\right)^{0.45}\right]\left(\frac{M_{crd}}{M_y}\right)^{0.45} M_y \tag{26}$$

$$\text{for } \lambda_{d1} < \lambda_d \leq \lambda_{d2}$$

$$M_{nd} = 0.88\left[1 - 0.2\left(\frac{M_{crd}}{M_y}\right)^{0.45}\right]\left(\frac{M_{crd}}{M_y}\right)^{0.45} M_y \qquad \text{for } \lambda_d > \lambda_{d2} \tag{27}$$

$$\lambda_{d1} = 0.538\left(\frac{M_{ynet}}{M_y}\right)^3 \tag{28}$$

$$\lambda_{d2} = 0.538\left[1.7\left(\frac{M_y}{M_{ynet}}\right)^{2.7} - 0.7\right] \tag{29}$$

$$M_{d2} = 0.88\left(1 - 0.2\left(\frac{1}{\lambda_{d2}}\right)^{0.9}\right)\left(\frac{1}{\lambda_{d2}}\right)^{0.9} M_y \tag{30}$$

$$M_{ni} = M_{ynet} \qquad \text{for } \lambda_l \leq \lambda_a \tag{31}$$

$$M_{nl} = \alpha\left[1 - 0.15\left(\frac{M_{crl}}{M_{ne}}\right)^{0.4\beta}\right]\left(\frac{M_{crl}}{M_{ne}}\right)^{0.4\beta} M_{ne} \leq M_{ynet} \qquad \text{for } \lambda_l > \lambda_a \tag{32}$$

$$\alpha = \left(\frac{M_{ynet}}{M_y}\right)^{19.4\left(\frac{M_{ynet}}{M_y}\right) - 14.8} \tag{33}$$

$$\beta = \left(\frac{M_{ynet}}{M_y}\right)^{2.1} \tag{34}$$

$$\lambda_a = Solution\ of\ the\ equation\ \frac{\alpha\left(1 - \frac{0.15}{{\lambda_a}^{0.8\beta}}\right)}{{\lambda_a}^{0.8\beta}} = \frac{M_{ynet}}{M_y} \tag{35}$$

Where, M_{nd} – section moment capacity for distortional buckling; M_{ynet}- member yield moment of net cross-section; M_{crd}- critical elastic distortional buckling moment (including the effect of web openings; M_y- member yield moment; λ_{d1}, λ_d and λ_{d2} - non-dimensional slenderness values

However, suitability of existing design equations to calculate the section moment capacity of SupaCee sections with web openings was not taken into consideration in the literature. Hence, it is necessary to check the reliability of existing equations to predict the flexural strengths of SupaCee sections with web openings.

6 Design approach for SupaCee sections with web openings

Extensive numerical study was carried out herein to examine the flexural performance of SupaCee sections with web openings. Since the lateral restraints were used in the compression flange of the SupaCee beam for whole section, failure of the section was prominently local buckling. Hence, this section reviews the validity of existing design equation to predict the flexural capacity of SupaCee section without web openings considering the condition of local buckling and introduce new design provisions to calculate the ultimate section moment capacity of SupaCee sections with web openings.

Pham and Hancock [3] stated that existing design equations (Eqn. (1) – (3)) were applicable to predict the flexural capacity of SupaCee sections at local buckling as they compared the experiment results with existing equations. Moreover, the researchers [3] investigated the flexural behaviour of SupaCee section with three different cases by changing the limiting moments. Limiting moments of those three cases were yield (M_y), inelastic (M_{ny}), and plastic (M_p) moments, which were defined as Case A, Case B, and Case C respectively in their study. Also, Pham and Hancock [3] proposed Case D with inelastic moment (M_{ny}). However, Case C (using M_p instead of M_{ne}) predicted well the local buckling failure of SupaCee sections. Hence, FE results were compared with proposed DSM-based equation based on Case C. For the comparison of FE results with prediction of Pham and Hancock [3] study, Thin-Wall 2.0 [53], finite strip analysis software was employed to determine the second moment area (I_X) and critical elastic buckling moment (M_{crl}) of those sections. Signature curve and buckling modes of SupaCee section is shown in Fig.19. The comparison of FE results with DSM equation displayed good agreement with the mean value of 1.00 and COV value of 0.08. Fig.20 demonstrates the comparison of FE results with existing design equation and experimental results of Pham and Hancock [3] study.

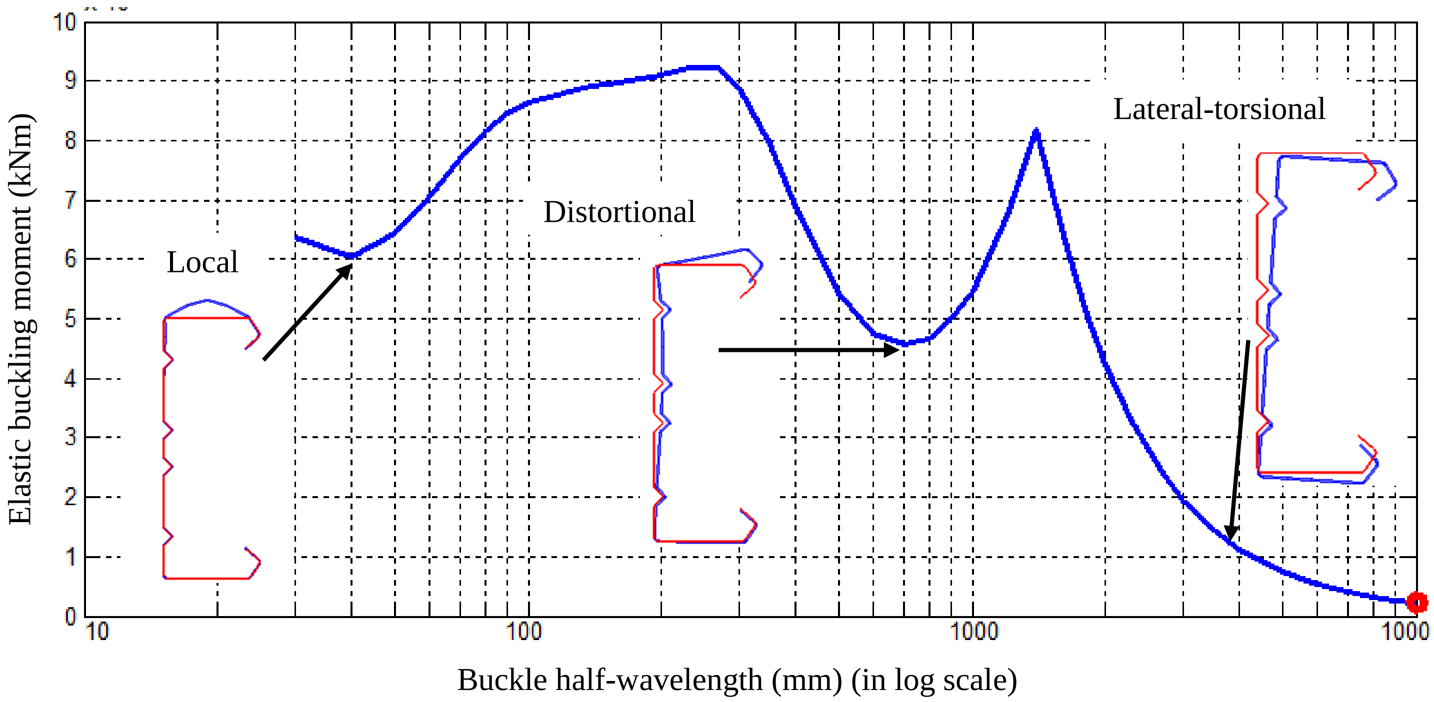

Fig.19: Signature curve and buckle modes of SupaCee section

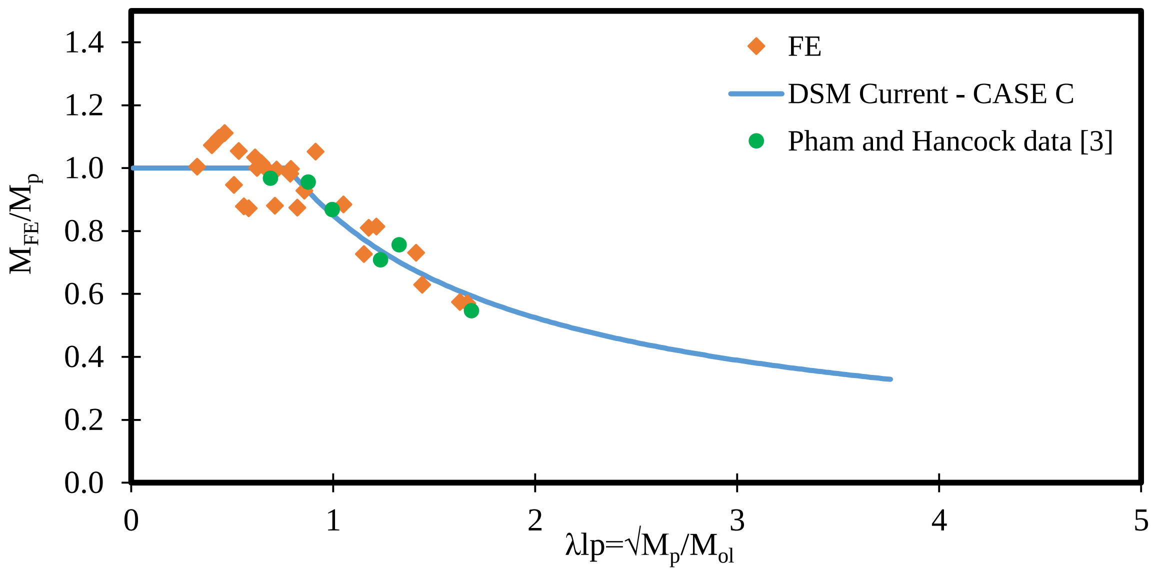

Fig.20: FE results comparison with DSM equation [3]

Based on the FE results comparison with current DSM equation, it can be concluded that existing design equation is applicable to predict the section moment capacity of SupaCee sections without web openings under local buckling condition. However, web opening reduces flexural capacity of SupaCee section, which should be investigated further and predicted using design equations.

Moen and Schafer [15] and Zhao et al. [16] proposed design equations to predict the flexural capacity of CFS sections with web openings. The researchers modified the DSM equations to account the reduction causes due to the openings. Since the method was more complex [21], a simple approach was developed by proposing reduction factors (q_s). Hence, reduction factor design equations (Eqs. (35) – (37)) were proposed herein considering the key parameters such as web opening ratio (d_{wh}/d_1) and hole spacing (s) based on the parametric results. Therefore, ultimate bending capacity of SupaCee sections with openings can be predicted by applying the proposed reduction factors to their corresponding bending capacity of solid sections, the bending capacity of solid sections can be determined using DSM equations. Besides, the comparison of proposed reduction factor equations with numerical results matched well with the mean value of 1.00 and COV value of 0.11. Fig.21 exhibits the good agreement of proposed equation with FE results. Moreover, reliability analysis was conducted for the proposed Eqs.36&37. From the reliability analysis, reduction factor (ϕ_b) of 0.87 is recommended to apply with the proposed equations.

$$M_{Opening} = M_{solid} \times q_s \tag{35}$$

$$q_s = 0.76 - \left(\frac{d_{wh}}{d_1}\right)^{0.31} + \left(\frac{s}{d_1}\right)^{-0.13} \quad for 0 < \frac{d_{wh}}{d_1} \leq 0.6 \tag{36}$$

$$q_s = 0.75 - \left(\frac{d_{wh}}{d_1}\right)^{0.43} + \left(\frac{s}{d_1}\right)^{-0.32} \quad for 0.6 < \frac{d_{wh}}{d_1} \leq 0.8 \tag{37}$$

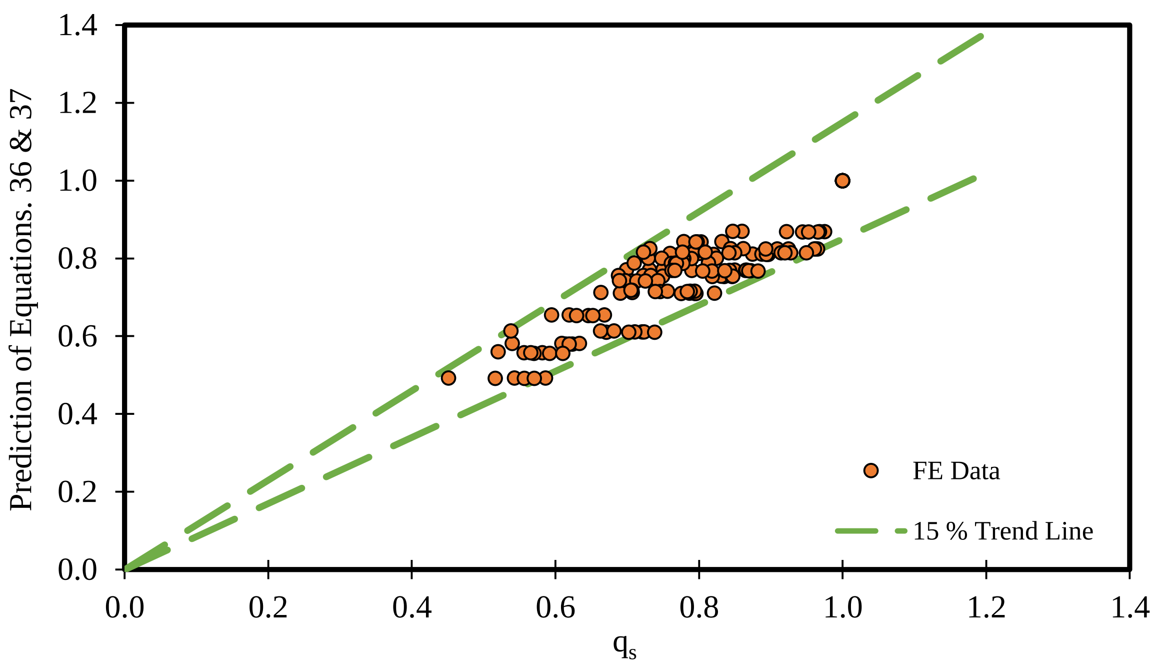

Fig.21: Comparison of proposed reduction factor equation with numerical

7 Comparison of results with LCB sections

This section reviews the applicability of SupaCee sections in the industry, by comparing the flexural performance of SupaCee sections with similar LCB sections. Therefore, LCB sections were modelled with the similar dimensions of SupaCee section and numerical analysis was conducted under similar terms. Fig.22 shows the considered dimensions for this comparative study. Altogether, 27 models were created incorporating the key parameters such as thickness (1 mm, 2 mm and 2.5 mm), yield strength (300 MPa, 450 MPa and 600 MPa) and sections; depth x width (150×50, 200×65 and 250×75). Results for LCB were obtained and compared with plain SupaCee sections.

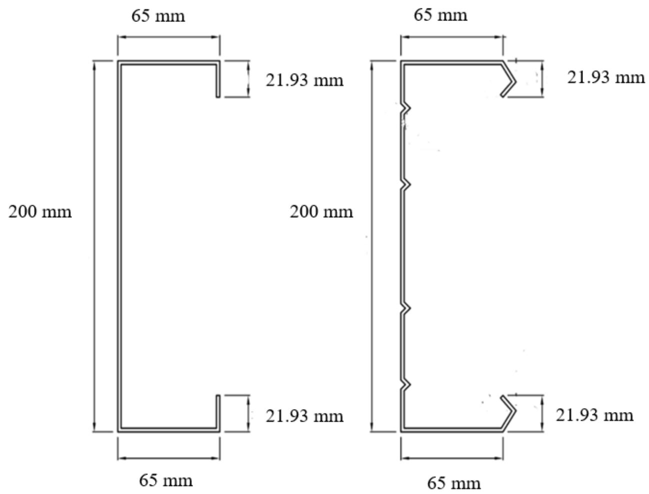

Fig.22: Comparison of dimensions of LCB and SupaCee section

Table.6 presents the flexural capacity comparison between SupaCee and LCB sections. Results clearly indicated better flexural performance of SupaCee sections; similar statement was reported earlier by Pham and Hancock [3] based on their experimental results. Moreover, flexural capacity enhancement of SupaCee section compared to LCB was recorded maximum of 89.79% and the least was 12.46%. Hence, the application of SupaCee sections in the industry should be considered as a potential initiative for mass production.

Table.6: Flexural capacity comparison of SupaCee sections with Similar LCB

Section depth	t	f_y	Section moment capacity (kNm)		Section moment capacity increment (%)
(mm)	(mm)	(MPa)	LCB	SupaCee	
150	1	300	2.47	4.12	66.80
150	2	300	6.3	9.05	43.65

150	2.5	300	7.9	10.01	26.71
150	1	450	3.65	5.89	61.37
150	2	450	10.11	13.05	29.08
150	2.5	450	12.8	16.04	25.31
150	1	600	4.6	7.23	57.17
150	2	600	13.42	17.07	27.20
150	2.5	600	17.28	22.15	28.18
200	1	300	3.38	6.04	78.70
200	2	300	9.55	12.98	35.92
200	2.5	300	12.31	17.05	38.51
200	1	450	4.8	9.11	89.79
200	2	450	15.05	21.89	45.45
200	2.5	450	19.05	27.05	41.99
200	1	600	5.58	9.54	70.97
200	2	600	18.59	29.02	56.11
200	2.5	600	23.35	35.89	53.70
250	1	300	5.08	9.55	87.99
250	2	300	16.94	19.05	12.46
250	2.5	300	21.9	26.08	19.09
250	1	450	6.76	11.11	64.35
250	2	450	24.85	28.85	16.10
250	2.5	450	32.27	38.4	19.00
250	1	600	8.35	13.44	60.96
250	2	600	30.27	38.2	26.20
250	2.5	600	40.86	54.02	32.21

In addition, flexural performances of Plain LCB was compared to the SupaCee sections with web openings to check the possibilities of replacement of LCB by SupaCee beam with additional advantage of web openings for service integration. Table.7 reports the ultimate flexural capacity comparison of LCB with SupaCee beam with web opening (web opening ratio of 0.4 and 0.6). Results from numerical models exhibited the possibilities for replacing LCB with SupaCee section with web openings (d_{wh}/d_1 = 0.4 and 0.6). For all sections, the observations were positive, as the section moment capacity of SupaCee section for both web opening ratios was better than the LCB. Considering the overall results and based on the situations, SupaCee sections with web openings (up to minimum web opening ratio of 0.6) can be a practicable option to replace the LCB. Fig.23 demonstrates the replacement options of SupaCee sections with openings for LCB in terms of flexural capacity comparisons. It indicates that replacement options for section 150 and section 200. Similarly, Fig.24 compares the flexural capacities of section 250 for checking replacement opportunities of SupaCee sections with LCB for different yield strength. For section 250, LCB can be replaced by SupaCee section with web opening ratio of up to 0.8. Hence, based on the flexural capacity comparison SupaCee section can be utilised in the industry to replace conventional CFS sections with an additional advantage of web opening.

Table.7: Comparison of section moment capacities of LCB with Supacee section with openings

Section depth	t	f_y	Section moment capacity (kNm)			Comparison with LCB section (%) ($M_{SupaCee\ with\ web\ opening}$ - M_{LCB})/ M_{LCB} * 100	
(mm)	(mm)	(MPa)	LCB	d_{wh}/d_1 = 0.4	d_{wh}/d_1 = 0.6	d_{wh}/d_1 = 0.4	d_{wh}/d_1 = 0.6
150	1	300	2.47	2.95	2.83	19.43	14.57
150	2	300	6.3	7	6.78	11.11	7.62
150	2.5	300	7.9	8.69	8.36	10.00	5.82
150	1	450	3.65	4.48	4.26	22.74	16.71
150	2	450	10.11	11.41	10.84	12.86	7.22
150	2.5	450	12.8	14.38	13.57	12.34	6.02
150	1	600	4.6	5.73	5.3	24.57	15.22
150	2	600	13.42	15.15	14.46	12.89	7.75
150	2.5	600	17.28	19.79	18.13	14.53	4.92
200	1	300	3.38	4.14	4.05	22.49	19.82
200	2	300	9.55	10.8	10.56	13.09	10.58
200	2.5	300	12.31	13.69	12.98	11.21	5.44
200	1	450	4.8	5.88	5.77	22.50	20.21
200	2	450	15.05	17.05	16.8	13.29	11.63
200	2.5	450	19.05	21.57	21.03	13.23	10.39
200	1	600	5.58	6.93	5.89	24.19	5.56
200	2	600	18.59	21.25	20.6	14.31	10.81
200	2.5	600	23.35	28.57	27.58	22.36	18.12
250	1	300	5.08	7.01	6.9	37.99	35.83
250	2	300	16.94	18.57	18.09	9.62	6.79
250	2.5	300	21.9	24.63	23.85	12.47	8.90
250	1	450	6.76	9.55	8.98	41.27	32.84
250	2	450	24.85	27.92	26.77	12.35	7.73
250	2.5	450	32.27	37.08	35.31	14.91	9.42
250	1	600	8.35	11.39	10.44	36.41	25.03
250	2	600	30.27	35.22	32.46	16.35	7.23
250	2.5	600	40.86	51.46	45.46	25.94	11.26

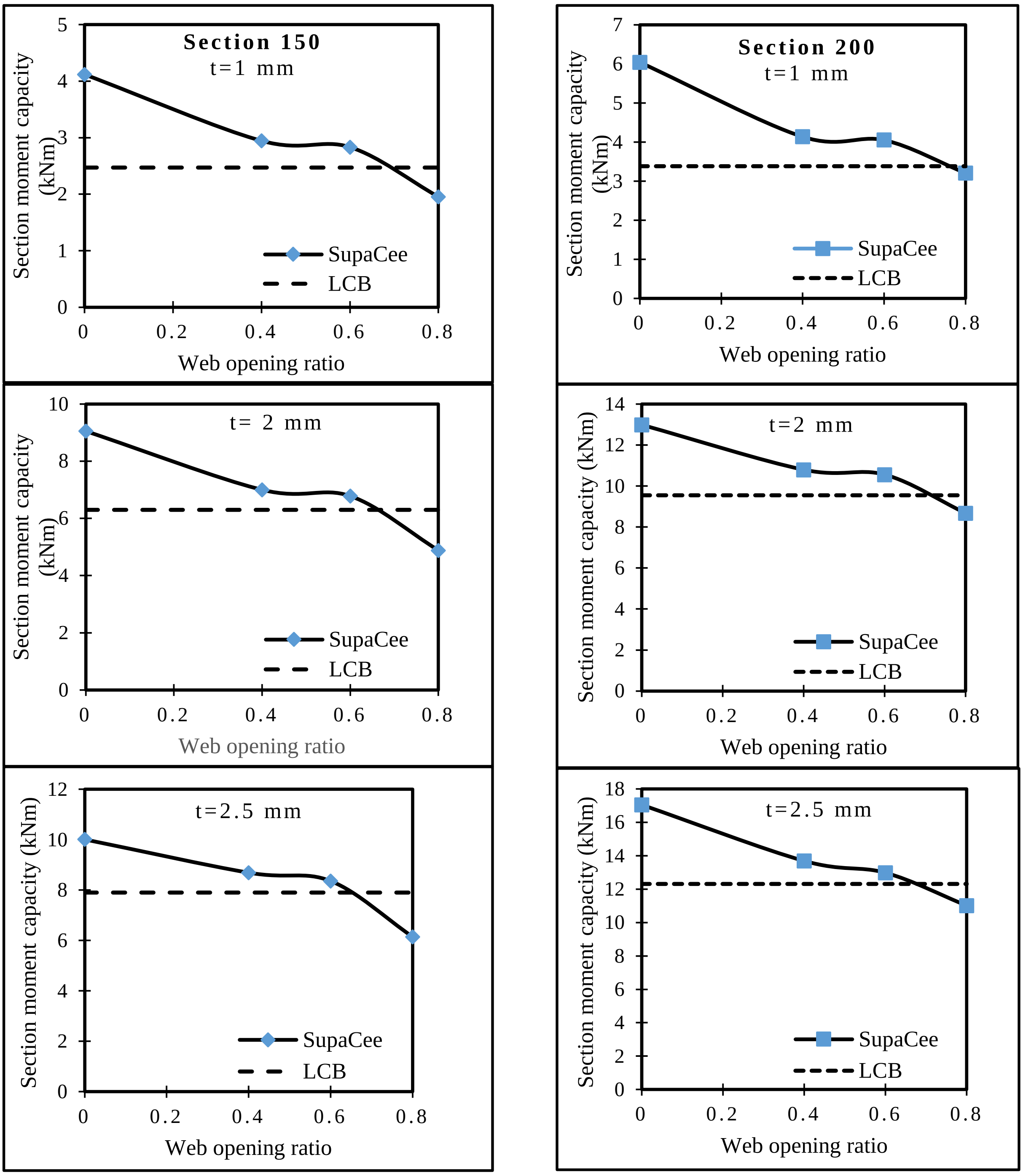

Fig.23: Flexural capacity comparison between LCB and SupaCee section with holes (f_y = 300 MPa) for different thicknesses

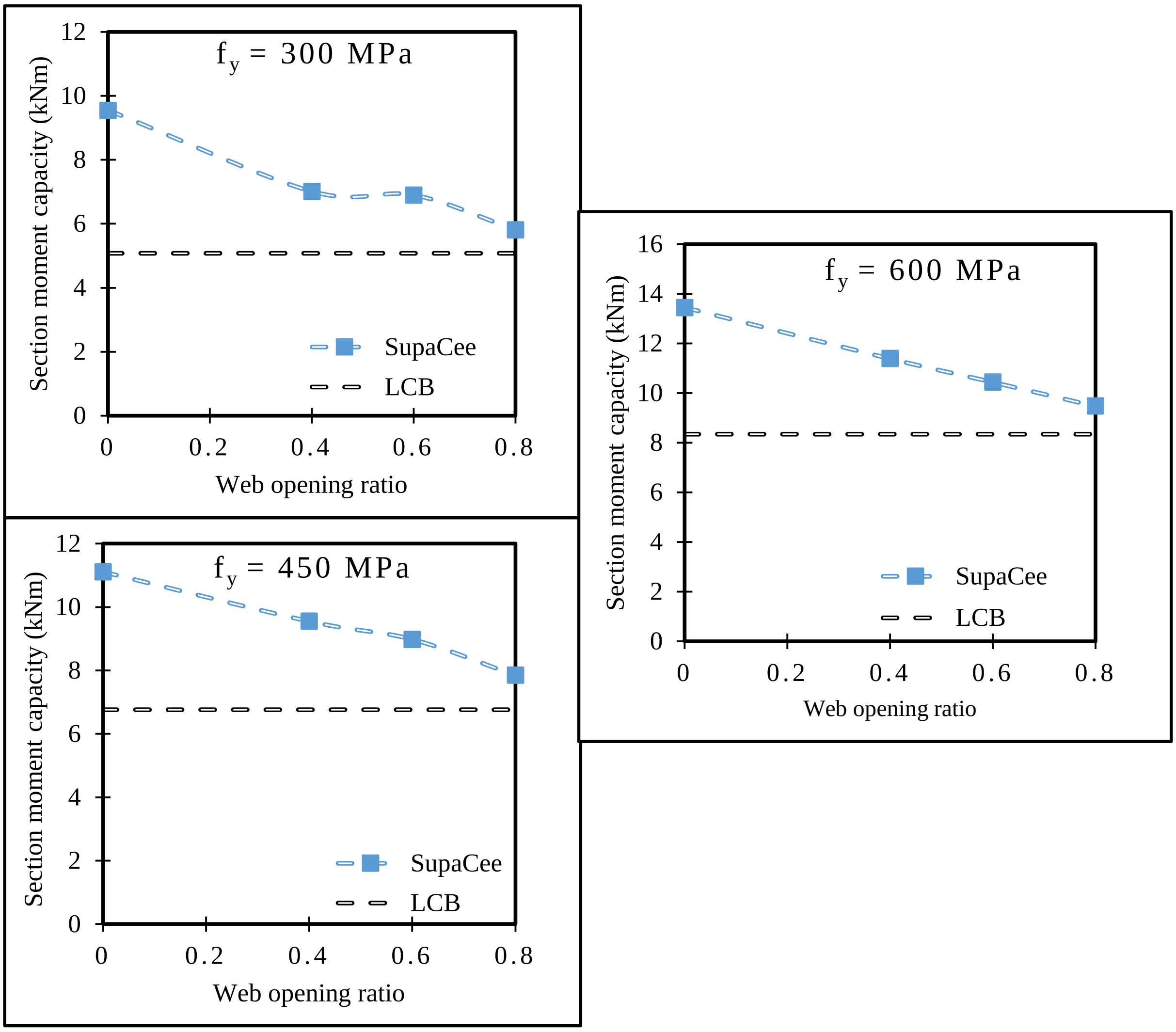

Fig.24: Flexural capacity comparison between LCB and SupaCee section with holes for section 250 (thickness = 1 mm)

8 Conclusion

This paper has reported a detailed investigation on flexural performance of SupaCee sections with web openings. Numerical analysis was initiated with validation followed by the implementation of parametric plan covering wide range of key parameters. Results were analysed while comparisons and recommendations were stated for considered key parameters. Since hole spacing was not considered in previous studies as a key parameter to format an equation to predict the ultimate bending moment, existing design equations are found inappropriate to compare the FE results. Hence, based on the numerical results new design provisions were proposed to predict the ultimate flexural capacities of SupaCee sections with web openings under predominantly local buckling failure scenario. Further, LCB sections were modelled to similar to SupaCee sections and ultimate flexural capacity of both LCB and

SupaCee sections with and without web openings were compared. Comparison displayed about 12.46 – 89.79 % enhancement in flexural capacity in plain SupaCee sections. Besides, better flexural capacities were observed in SupaCee section with web openings (beyond web opening ratio of 0.6) compared to LCB. Hence, this paper recommends the practical application of SupaCee sections as a replacement of conventional CFS sections including LCB with an additional advantage of having web openings for service integrations considering the comparison of flexural performance. Overall, this study concludes that proposed design equations do accurately predict the flexural capacity of SupaCee sections with web openings and recommends design considerations and applicability of SupaCee section with web openings in the industry. However, since the study was conducted using numerical approaches purely, the proposed equations could be verified with experimental results for more accuracy.

9 Acknowledgements

The authors would like to acknowledge the supports provided by the Northumbria University, European research council and The Home Engineers.

References

[1] P. Gatheeshgar, K. Poologanathan, S. Gunalan, K. D. Tsavdaridis, B. Nagaratnam, and E. Iacovidou, "Optimised cold-formed steel beams in modular building applications," *J. Build. Eng.*, vol. 32, p. 101607, 2020.

[2] P. C. Hung, B. L. A., and G. J. Hancock, "Experimental Study of Longitudinally Stiffened Web Channels Subjected to Combined Bending and Shear," *J. Struct. Eng.*, vol. 141, no. 11, p. 4015018, Nov. 2015.

[3] P. C. Hung and G. J. Hancock, "Experimental Investigation and Direct Strength Design of High-Strength, Complex C-Sections in Pure Bending," *J. Struct. Eng.*, vol. 139, no. 11, pp. 1842–1852, Nov. 2013.

[4] B. Chen, K. Roy, A. Uzzaman, and J. B. P. Lim, "Moment capacity of cold-formed channel beams with edge-stiffened web holes, un-stiffened web holes and plain webs," *Thin-Walled Struct.*, vol. 157, p. 107070, 2020.

[5] "Service holes for plumbing and electrical - Spantec." [Online]. Available: https://spantec.com.au/products/boxspan-upper-floor-frames/upper-floor-gallery/olympus-digital-camera-4/. [Accessed: 04-Jan-2022].

[6] "Service integration - SteelConstruction.info." [Online]. Available: https://www.steelconstruction.info/Service_integration. [Accessed: 04-Jan-2022].

[7] Y. Cheng and S. B. W., "Distortional Buckling Tests on Cold-Formed Steel Beams," *J. Struct. Eng.*, vol. 132, no. 4, pp. 515–528, Apr. 2006.

[8] C. Yu and B. W. Schafer, "Simulation of cold-formed steel beams in local and distortional buckling with applications to the direct strength method," *J. Constr. Steel Res.*, vol. 63, no. 5, pp. 581–590, 2007.

[9] C. Yu and W. Yan, "Effective Width Method for determining distortional buckling strength of cold-formed steel flexural C and Z sections," *Thin-Walled Struct.*, vol. 49, no. 2, pp. 233–238, 2011.

[10] N. Dolamune Kankanamge and M. Mahendran, "Behaviour and design of cold-formed steel beams subject to lateral–torsional buckling," *Thin-Walled Struct.*, vol. 51, pp. 25–38, 2012.

[11] M. Anbarasu, "Local-distortional buckling interaction on cold-formed steel lipped channel beams," *Thin-Walled Struct.*, vol. 98, pp. 351–359, 2016.

[12] M. R. Haidarali and D. A. Nethercot, "Finite element modelling of cold-formed steel beams under local buckling or combined local/distortional buckling," *Thin-Walled Struct.*, vol. 49, no. 12, pp. 1554–1562, 2011.

[13] L. Wang and B. Young, "Design of cold-formed steel channels with stiffened webs subjected to bending," *Thin-Walled Struct.*, vol. 85, pp. 81–92, 2014.

[14] P. Gatheeshgar, S. Parker, K. Askew, K. Poologanathan, S. Navaratnam, A. McIntosh, and D. Widdowfield Small, "Flexural behaviour and design of modular construction optimised beams," *Structures*, vol. 32, pp. 1048–1068, 2021.

[15] C. D. Moen and B. W. Schafer, "Elastic buckling of cold-formed steel columns and beams with holes," *Eng. Struct.*, vol. 31, no. 12, pp. 2812–2824, 2009.

[16] J. Zhao, K. Sun, C. Yu, and J. Wang, "Tests and direct strength design on cold-formed steel channel beams with web holes," *Eng. Struct.*, vol. 184, pp. 434–446, 2019.

[17] N. Yu, B. Kim, W. Yuan, L. Li, and F. Yu, "An analytical solution of distortional

buckling resistance of cold-formed steel channel-section beams with web openings," *Thin-Walled Struct.*, vol. 135, pp. 446–452, 2019.

[18] G. J. Hancock, "Design for distortional buckling of flexural members," *Thin-Walled Struct.*, vol. 27, no. 1, pp. 3–12, 1997.

[19] T. K. Daniel and D. Cedric, "Vierendeel Bending Study of Perforated Steel Beams with Various Novel Web Opening Shapes through Nonlinear Finite-Element Analyses," *J. Struct. Eng.*, vol. 138, no. 10, pp. 1214–1230, Oct. 2012.

[20] N. Degtyareva, P. Gatheeshgar, K. Poologanathan, S. Gunalan, K. D. Tsavdaridis, and S. Napper, "New distortional buckling design rules for slotted perforated cold-formed steel beams," *J. Constr. Steel Res.*, vol. 168, p. 106006, 2020.

[21] N. Degtyareva, P. Gatheeshgar, K. Poologanathan, S. Gunalan, I. Shyha, and A. McIntosh, "Local buckling strength and design of cold-formed steel beams with slotted perforations," *Thin-Walled Struct.*, vol. 156, p. 106951, 2020.

[22] K. Poologanathan and M. Mahendran, "New Design Rules for the Shear Strength of LiteSteel Beams with Web Openings," *J. Struct. Eng.*, vol. 139, no. 5, pp. 640–656, May 2013.

[23] K. S. Wanniarachchi, M. Mahendran, and P. Keerthan, "Shear behaviour and design of Lipped Channel Beams with non-circular web openings," *Thin-Walled Struct.*, vol. 119, pp. 83–102, 2017.

[24] P. Keerthan and M. Mahendran, "Experimental studies of the shear behaviour and strength of lipped channel beams with web openings," *Thin-Walled Struct.*, vol. 73, pp. 131–144, 2013.

[25] P. Keerthan and M. Mahendran, "Improved shear design rules for lipped channel beams with web openings," *J. Constr. Steel Res.*, vol. 97, pp. 127–142, 2014.

[26] P. Keerthan and M. Mahendran, "Shear Behaviour and Strength of LiteSteel Beams with Web Openings," *Adv. Struct. Eng.*, vol. 15, no. 2, pp. 171–184, Feb. 2012.

[27] D. L. Chandramohan, E. Kanthasamy, P. Gatheeshgar, K. Poologanathan, M. F. M. Ishqy, T. Suntharalingam, and T. Kajaharan, "Shear behaviour and design of doubly symmetric hollow flange beam with web openings," *J. Constr. Steel Res.*, vol. 185, p.

106836, 2021.

[28] H. Sun, B. Cao, Z. Chen, and Y. Du, “Shear behaviour of reinforced straw-bale plaster sheathed cold-formed steel-framed shear walls,” *Biosyst. Eng.*, vol. 221, pp. 54–68, 2022.

[29] N. Degtyareva, P. Gatheeshgar, K. Poologanathan, S. Gunalan, M. Lawson, and P. Sunday, “Combined bending and shear behaviour of slotted perforated steel channels: Numerical studies,” *J. Constr. Steel Res.*, vol. 161, pp. 369–384, 2019.

[30] M. F. M. Ishqy, S. Wanniarachchi, and K. Poologanathan, “Shear behaviour of screw fastened rectangular hollow flange beams with web openings,” *J. Constr. Steel Res.*, vol. 189, p. 107019, 2022.

[31] K. Thirunavukkarasu, E. Kanthasamy, K. Poologanathan, K. D. Tsavdaridis, P. Gatheeshgar, S. Hareindirasarma, and A. McIntosh, “Shear performance of SupaCee sections with openings: Numerical studies,” *J. Constr. Steel Res.*, vol. 190, p. 107142, 2022.

[32] H. Alsanat, S. Gunalan, P. Gatheeshgar, K. Poologanathan, and A. M. Thabet, “Design of roll-formed aluminium lipped channel sections with web opening subjected to web crippling under end-two-flange load case,” *J. Build. Eng.*, vol. 48, p. 103887, 2022.

[33] A. McIntosh, P. Gatheeshgar, S. Gunalan, E. Kanthasamy, K. Poologanathan, M. Corradi, and C. Higgins, “Unified approach for the web crippling design of cold-formed channels: Carbon steel, stainless steel and aluminium,” *J. Build. Eng.*, vol. 51, p. 104134, 2022.

[34] Z. Fang, K. Roy, J. Xu, Y. Dai, B. Paul, and J. B. P. Lim, “A novel machine learning method to investigate the web crippling behaviour of perforated roll-formed aluminium alloy unlipped channels under interior-two flange loading,” *J. Build. Eng.*, vol. 51, p. 104261, 2022.

[35] P. Keerthan, M. Mahendran, and E. Steau, “Experimental study of web crippling behaviour of hollow flange channel beams under two flange load cases,” *Thin-Walled Struct.*, vol. 85, pp. 207–219, 2014.

[36] K. Elilarasi, S. Kasthuri, and B. Janarthanan, “Effect of circular openings on web

crippling of unlipped channel sections under end-two-flange load case," *Adv. Steel Constr.*, vol. 16, no. 4, pp. 310–320, 2020.

[37] K. Thirunavukkarasu, E. Kanthasamy, P. Gatheeshgar, K. Poologanathan, S. Das, S. Todhunter, and T. Suntharalingam, "Web crippling design of modular construction optimised beams under ETF loading," *J. Build. Eng.*, vol. 43, p. 103072, 2021.

[38] S. Hareindirasarma, K. Elilarasi, and B. Janarthanan, "Effect of circular holes on the web crippling capacity of cold-formed LiteSteel beams under Interior-Two-Flange load case," *Thin-Walled Struct.*, vol. 166, p. 108135, 2021.

[39] K. Elilarasi and B. Janarthanan, "Effect of web holes on the web crippling capacity of cold-formed LiteSteel beams under End-Two-Flange load case," *Structures*, vol. 25, pp. 411–425, 2020.

[40] P. Gatheeshgar, H. Alsanat, K. Poologanathan, S. Gunalan, N. Degtyareva, S. Wanniarachchi, and I. Fareed, "Web crippling of slotted perforated Cold-Formed Steel channels under EOF load case: Simulation and design," *J. Build. Eng.*, vol. 44, p. 103306, 2021.

[41] P. Gatheeshgar, H. Alsanat, K. Poologanathan, S. Gunalan, N. Degtyareva, and I. Hajirasouliha, "Web crippling behaviour of slotted perforated cold-formed steel channels: IOF load case," *J. Constr. Steel Res.*, vol. 188, p. 106974, 2022.

[42] K. D. Tsavdaridis and C. D'Mello, "Web buckling study of the behaviour and strength of perforated steel beams with different novel web opening shapes," *J. Constr. Steel Res.*, vol. 67, no. 10, pp. 1605–1620, 2011.

[43] K. D. Tsavdaridis and G. Galiatsatos, "Assessment of cellular beams with transverse stiffeners and closely spaced web openings," *Thin-Walled Struct.*, vol. 94, pp. 636–650, 2015.

[44] Dassault Systems Simulia Corp, "Abaqus/CAE 2017 User's Guide," *Abaqus/CAE Standard 2017*. 2017.

[45] C. H. Pham and G. J. Hancock, "Numerical simulation of high strength cold-formed supacee® sections in combined bending and shear," *Res. Rep. - Univ. Sydney, Dep. Civ. Eng.*, no. 913, 2010.

[46] Thirunavukkarasu K, Kanthasamy E, Gatheeshgar P, Poologanathan K, Rajanayagam H, Suntharalingam T, Dissanayake M. Sustainable Performance of a Modular Building System Made of Built-Up Cold-Formed Steel Beams. *Buildings*. 2021; 11(10):460.

[47] N. Perera and M. Mahendran, “Finite element analysis and design for section moment capacities of hollow flange steel plate girders,” *Thin-Walled Struct.*, vol. 135, pp. 356–375, 2019.

[48] E. Kanthasamy, K. Thirunavukkarasu, K. Poologanathan, P. Gatheeshgar, S. Todhunter, T. Suntharalingam, and M. Fareedh Muhammadh Ishqy, “Shear behaviour of doubly symmetric rectangular hollow flange beam with circular edge-stiffened openings,” *Eng. Struct.*, vol. 250, p. 113366, 2022.

[49] B. W. Schafer, Z. Li, and C. D. Moen, “Computational modeling of cold-formed steel,” *Thin-Walled Struct.*, vol. 48, no. 10, pp. 752–762, 2010.

[50] American Iron and Steel Institute (AISI), Specifications for the cold-formed steel structural members, cold-formed steel design manual, AISI S100, Washington DC, USA; 2016.

[51] Australia/New Zealand Standard AS/NZS 4600 Cold-Formed Steel Structures, Standards Australia/Standards New Zealand (SA), Sydney, Australia, 2018.

[52] S. Yared and S. B. W., “Inelastic Bending Capacity of Cold-Formed Steel Members,” *J. Struct. Eng.*, vol. 138, no. 4, pp. 468–480, Apr. 2012.

[53] V.V. Nguyen, G.J. Hancock, C.H. Pham, Application of the THIN-WALL-2 V2.0 Program for Analysis of Thin-Walled Sections Under Localised Loading, Proceedings of the 4th Congr`es International de G´eotechnique - Ouvrages -Structures2018, pp. 78-88.